LAPPEENRANTA UNIVERSITY OF TECHNOLOGY
LUT School of Energy Systems
LUT Mechanical Engineering

*Mojtaba Mobaraki*

**INVESTIGATING HIGH-POWER ULTRASONIC VIBRATION AND VACUUM AS METHODS TO ENHANCE THE EXTRACTION OF WATER FROM MUNICIPAL WASTEWATER SLUDGE**

Examiners: Professor Aki Mikkola
Ph.D. R Scott Semken

**“If you wish to find the secrets of the universe, think in terms of Energy, Frequency, and Vibration."**

**Nikola Tesla**

## ABSTRACT

Lappeenranta University of Technology
LUT School of Energy Systems
LUT Mechanical Engineering

Mojtaba Mobaraki

**Investigating high-power ultrasonic vibration and vacuum as methods to enhance the extraction of water from municipal wastewater sludge**

Master's thesis

2016

97 pages, 62 figures, and 9 tables

Examiners: Professor Aki Mikkola
Ph.D. R Scott Semken

Keywords: high-power ultrasound, vibration, oscillation, resonance, dewatering, atomization, sponge effect, cavitation, micro-channels, mode shape, frequency, sludge, drying, vacuum, drying kinetics, pressure and displacement waves, sound intensity

The main objective of this thesis is to uncover and investigate physical mechanisms that can be used to develop efficient ways to remove water from municipal wastewater sludge. The essential criterion will be to minimize energy expenditure. For this purpose, the main theories regarding mechanical dewatering and drying, related methods, and normally available dewatering and drying machinery are discussed.

Using vacuum to enhance drying and applying high-power ultrasound to enhance dewatering or drying are two areas of particular interest. The potential advantage of vacuum is discussed in brief, and a series of experiments performed to investigate its effect on drying kinetics are described. To introduce high-power ultrasound, some basic theoretical data about vibration translation, standing waves, and air columns in musical instruments are presented. Then, the basic mechanisms and equipment of ultrasonic processing related to water extraction technologies are discussed. Finally, testing was carried out at the Pusonics Co. in Spain to explore the use of ultrasonic waves for dehydration.

The investigation and testing show that both vacuum-enhanced drying and high-power ultrasound-enhanced dewatering or drying could be used to develop more effective and more energy efficient ways of removing water from municipal wastewater sludge.

**ACKNOWLEDGEMENTS**

First, I sincerely would like to thank my supervisor Prof. Aki Mikkola for providing me with the valuable opportunity to join his outstanding team to pursue my master thesis. Next, my special thanks to my adviser Dr. R Scott Semken for all of his supports, helps, and advices over this work.

I am grateful to thank all the Machine Design Lab members for their friendship and helps, specially Marko Matikainen, John Bruzzo Escalante, and Grzegorz Orzechowski.

I want to thank my family particularly my parents Mr. Hassan and Mrs. Marzieh Mobaraki also my siblings, all the supports you have provided me over the years was the greatest gift anyone has ever given me and thanks for your love and support while we are thousand kilometers away from you.

Finally, My thanks to my wife Hanieh and my little son Erfan for their patience over the last years as I have concentrated on the work.

*Mojtaba Mobaraki*

Lappeenranta 9.6.2016

*Dedicated to my dear mother*

**TABLE OF CONTENTS**

## LIST OF SYMBOLS AND ABBREVIATIONS

| | |
|---|---|
| $A$ | Surface of filter area [m2] |
| $a$ | Amplitude [m] |
| $A_s$ | Surface area of sound sphere propagation field [m2] |
| $B$ | Bulk modulus [Pa] |
| $f$ | Frequency [1/s , Hz] |
| $g$ | Earth gravitational acceleration [m/s2] |
| $G$ | Centrifugal force [N] |
| $I$ | Sound intensity [W/m2] |
| $I_0$ | Threshold of hearing [1.10-12 W/m2] |
| $L$ | Sludge cake thickness and air column length [m] |
| $P$ | Power [W] |
| $Q$ | Flow rate [m3/s] |
| $r$ | Radius of centrifugal vessel [m] |
| $R$ | Distance from the sound source [m] |
| $r_0$ | Radial distance of free water [m] |
| $Rb$ | Bubble radius [m] |
| $r_p$ | Capillary radius [m] |
| $r_s$ | Radial distance from sludge cake surface [m] |
| $S$ | Particle displacement or wave amplitude [m] |
| $T$ | Temperature in degrees of kelvin |
| $v$ | Wave or sound speed [m/s] |
| $v_{air}$ | Velocity of sound in air [m/s] |
| | |
| $\mu$ | Water dynamics viscosity [N s/m2] |
| $\Gamma$ | Vibration intensity [m/s2] |
| $\gamma_{23}$ | Surface tension [N/m] |
| $\Delta P$ | Pressure drop inside the sludge cake [Pa] |
| $\theta$ | Angle between contact surfaces of solid-liquid-gas [°] |
| $\lambda$ | Wavelength [m] |
| $\rho$ | Density [kg/m3] |

| | |
|---|---|
| $\omega$ | Angular velocity [rad/s] |
| | |
| $c$ | Portion of particles in overflow |
| *Cth-1* | Coarse portion that flows over screen |
| $E$ | Combined effectiveness or overall efficiency |
| $f_b$ | Amount of particles bigger than the screen apertures |
| *Fth-1* | Feed material |
| gm | Gram |
| *I(dB)* | Intensity in decibel |
| $K$ | permeability of sludge cake |
| $n$ | The number of harmonic or mode shape |
| $P_p$ | Capillary pressure [Pa] |
| *Uth-1* | Fine part that passes through the screen |
| | |
| EPA | American Environmental Protection Agency |
| PS | Primary sludge |
| SS | Mixture of PS (Primary sludge) and WAS (waste activated sludge) |
| SSA | Specific surface area |
| TS | Totally solid |
| US | Ultrasound |
| WAS | Waste activated sludge or secondary sludge |
| WWTP | Wastewater treatment plant |

# 1 INTRODUCTION

The wastewater treatment process is for refining sewage water. The end products of this work are purified water and sewage sludge, which makes up the main byproduct of WWTP (wastewater treatment plant).

## 1.1 Sewage sludge problems

Human activities, both domestic and industrial, produce large amounts of residual sludge. The amount of dehydrated sludge produced each day is roughly between 0.2 to 0.3 kg (kilograms) per inhabitant. [1] Based on data collected from the year 2005, sludge production was about 7,600,000 dry metric ton/annum in the United States and 8,331,000 in the European Union [2]. It is estimated that sludge production for Europe will increase to 13,500,000 ton/ annum by the year 2020 [3].

One of the most cost effective sludge disposition methods is landfilling. However, sewage sludge contains heavy metals. Therefore, heavy metals can leach into the soil and enter the ecosystem, contaminating food materials and water. [4]

According to the requirements of the European Communities [5] "Sludge arising from waste water treatment shall be re-used whenever appropriate. Disposal routes shall minimize the adverse effects on the environment." By increasing the distribution of WWTP across the globe, the production of sewage sludge is increasing substantially. Furthermore, because of future restrictions on organic wastes landfilling, it is extremely critical to find methods to address this issue. [1]

## 1.2 Motivation

The energy production from dried sewage sludge has been becoming a common interest in many countries. Sewage sludge is classified as a renewable and environmentally friendly source of energy. [3] Correspondingly, in some cities, for example in London, electricity production from sewage sludge in different scales has already begun [6].

Energy production from sewage sludge has two main benefits: economic and environmental. From the environmental point of view, burning sewage sludge may produce less pollution than burning fossil fuel. Regarding economics, sludge can be a free and endless source of energy, and the dumping of sludge has recently been identified as polluting. Therefore countries should find a solution to eradicate the produced sludge from their WWTPs that costs itself, so by transforming it into energy they can save the expenses of sludge eradication beside the benefit of the resultant energy.

In many WWTPs, sewage sludge is translated to other places to dump under the ground (landfilling) or land spreading. Both of these approaches are encountering more legal restrictions and increasing transportation costs. According to EPA (American Environmental Protection Agency) estimates, the cost of sludge handling and disposal amounts to 40% – 60% of the total budget of WWPTs. [7]

When asked from the operators of WWTPs about the expenses of water treatment, most operators respond with sludge disposal expenses in euro per cubic meter, €/$m^3$. This price is mainly a function of water content. Higher water content equates to higher transportation expenses. In addition, to effectively burn sludge to produce energy production, its water content must be relatively low. It is critical to increase its TS (total solids) level. [7,8]

Dehydration history

Dehydration is an old technology that has been used for many years. One of the first reasons that human being started to use it, was for preservation purposes of food material, before the time that man had access to electricity and refrigerator [9].

The basic mechanisms for water extraction have remained unchanged for decades, and they are based on a few fundamental and simple principles such as gravity, pressure, filtration, and temperature. Endeavoring to uncover new dehydration mechanisms seems to be worthwhile.

PAKU+HERGE project

This work was undertaken as a part of the PAKU+HERGE project seeking technologies that could be used to improve the management of municipal sludge with the main target of

producing electricity from the residual sludge of municipal WWTP. The work has three main steps: (A) Dewatering and drying the resultant sludge from WWTP, (B) Burning the product of the dehydration process, and (C) Producing electricity from the produced heat energy.

This thesis describes work carried out as part of the first step, section (A) that is a thorough investigation of different dewatering and drying technologies, in particular mechanical methods. The main objective at this work is to find a new state of the art mechanical method to enhance dewatering.

To burn sludge efficiently, it is needed to decrease its water content percentage, because sludge with high water content cannot be burned efficiently. The energy needed to evaporate its water content prior to ignition consumes a great deal of energy. Figure 1 shows the relationship between sludge energy value and moisture content. Above all, the dehydration step itself should be cost effective. Therefore, one important criterion in this work is low energy water removal. Additionally, an efficient dehydration method can be served in many other areas like mining industry because dewatering is the key step before ore can be sent for further processing [10].

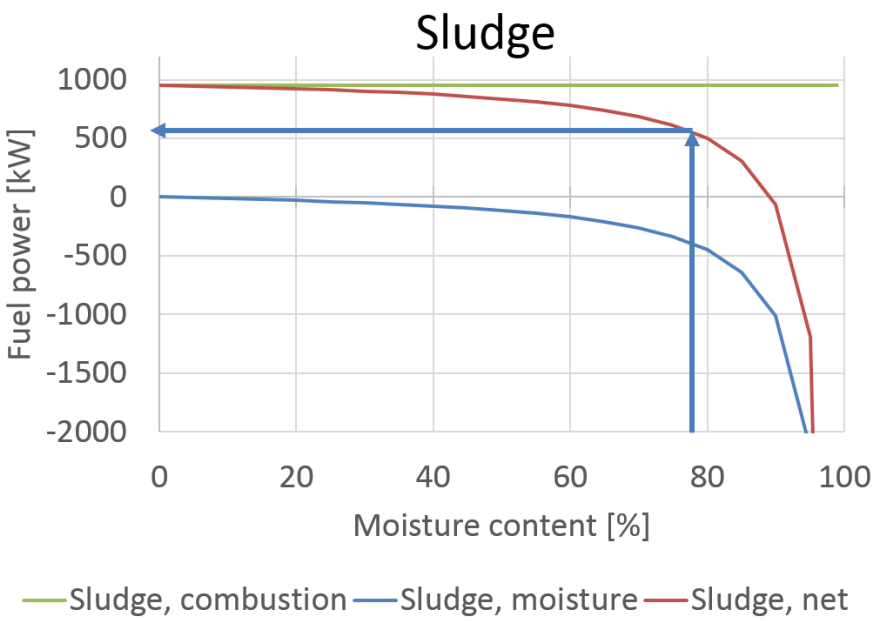


**Figure 1.** Sludge energy value and moisture content graph [11].

If the ultimate use of dry sludge is as a fuel for a furnace, vacuum can be used to lower the vaporization point of its water so it can be dried using the waste heat of the furnace. The

benefit of this work is that in vacuum drying there is no need to high temperature in drying process to maintain the drying kinetics. Therefore, with low temperature and sufficient amount of heat energy it could be possible to dry sludge in a reasonable span of time.

Outline of the thesis

First, to study the water extraction process some theories about dewatering and drying are presented. Effective factors of dewatering are discussed such as pressure difference (airflow) and screening that is a key issue in majority of water extraction methods in addition to an introduction of vibrating screens. Then some common dewatering machines for sludge dewatering are presented. From the energy consumption point of view, it comes out that dewatering is an economical process as well as a high-speed solution for water extraction.

Next to the dewatering materials are drying theories as thermal energy consumption under atmospheric and vacuum conditions, some data about few drying machines for sludge processing, and finally discussion about the energy consumption comparison between dewatering and drying that shows drying is extremely energy intensive method.

Successively is a chapter about theory of high frequency vibration and ultrasound. The content materials are standing waves theory, ultrasonic effective mechanisms in water extraction, ultrasonic equipment, and ultrasonic dehydration.

The next section is about the performed practical experiments of atmospheric and vacuum drying in addition to ultrasonic-assisted dehydration. At the end of this part, it is demonstrated that ultrasound could be a mechanical method which can extract the water content up to a high level without using heat energy, no other mechanical dewatering method is available that can perform dewatering like ultrasound.

## 1.3 Main achievement

One effective method for water extraction, that markedly enhances the dehydration kinetics and final TS, is using high frequency vibration or ultrasonic waves in both mechanical dewatering and thermal drying. To study the ultrasonic mechanisms phenomena, the physics of sound, air columns, and standing waves are investigated to explain the resultant harmonic mode shapes in the material subjected to an oscillatory exciter. In addition, effective

ultrasonic mechanisms such as atomization, sponge effect, cavitation, and micro channels propagation are explored.

Finally, an important weakness of ultrasonic mechanisms based on the physics of standing waves is found. The weakness, nodes of pressure and displacement waves, does not allow ultrasound to work evenly in all the material texture (based on the research conducted at this thesis, no document about this weakness was found). At the end, few methods are proposed to address this weakness of mechanisms.

# 2 THEORIES AND METHODS OF DEWATERING AND DRYING

In this research, the main material being processed is sludge. The material characteristics and the composition of sludge are subject to change with time, although the basic material remains nearly constant.

## 2.1 Sewage Sludge of WWTP

The main component of sludge from the municipal WWTP is water, something between 95 to 99%, and this high water content makes it too heavy for low-cost handling or transport. [12]

Sludge water content is divided into four main categories:

*Free Water:* This type of moisture is not attached to solid mater and can be easily removed via simple gravitational settling [12].

*Floc or Interstitial Water:* Floc water is the trapped moisture inside the flocs and is translated with flocs motion. It is possible to extract this type of water via mechanical dewatering. [12]

*Capillary or Surface Water:* This type of water content forms a thin layer on solid particles and attached to them, it can partially be squeezed out by mechanical dewatering [12].

*Particle or Bound Water:* This type of moisture content is attached, intracellularly and chemically, to solid particles. It is not possible to extract the bound water via known mechanical dewatering methods. Figure 2 shows the four types of water inside schematic sludge. [12]

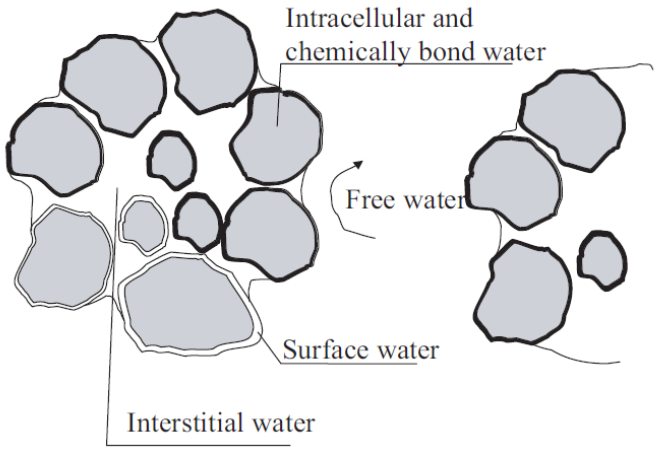


**Figure 2.** Four types of water inside sludge solid particles [13].

When industrial sewage is mixed up with domestic sewage the resultant is composed of organic substances (like fecal material, fibers, food wastes, biological flocs, and organic chemical components) [14]; and inorganic substances including heavy metals like cooper, lead, and zinc. [1] Table 1 lists the typical metal content composition of municipal sludge.

*Table 1. Typical metal content composition of municipal sludge* [13].

| Metal contents (mg/kg, dry basis) | Range | Median |
|---|---|---|
| Arsenic | 1.1–230 | 10 |
| Cadmium | 1–3410 | 10 |
| Chromium | 10–99 000 | 500 |
| Copper | 84–17 000 | 800 |
| Lead | 13–26 000 | 500 |
| Mercury | 0.6–56 | 6 |
| Molybdenum | 0.1–214 | 4 |
| Nickel | 2–5300 | 80 |
| Selenium | 1.7–17.2 | 5 |
| Zinc | 101–49 000 | 1700 |
| Iron | 1000–154 000 | 17 000 |
| Cobalt | 11.3–2490 | 30 |
| Tin | 2.6–329 | 14 |
| Manganese | 32–9870 | 260 |

Sludge types

The residual sludge from the WWTP is divided into three main categories: primary, secondary, and tertiary sludge. The sewage sludge for dehydration process can be any of these, or a combination of two, or all of them. [14]

Primary sludge is physically processed and achieved by simple gravitational settling at the beginning of the treatment process. See Figure 3. The level of TS in primary sludge is something between 2 to 7%. In comparison with the secondary and tertiary sludge, primary sludge can be dewatered and dried faster and easier because it is composed of discrete particles and debris.[14]

Secondary, biological, or activated sludge is the result of biological treatment. In this stage, bacteria consume both soluble and insoluble organics. The amount of TS is about 1.4 to 1.5%. Dewatering and drying secondary sludge is more difficult than dewatering and drying primary sludge, because of the light biological flocs from the biological treatment process. [14]

Tertiary, or chemically treated sludge is a combination of dissolved and suspended solids and the result of chemical processing [12].

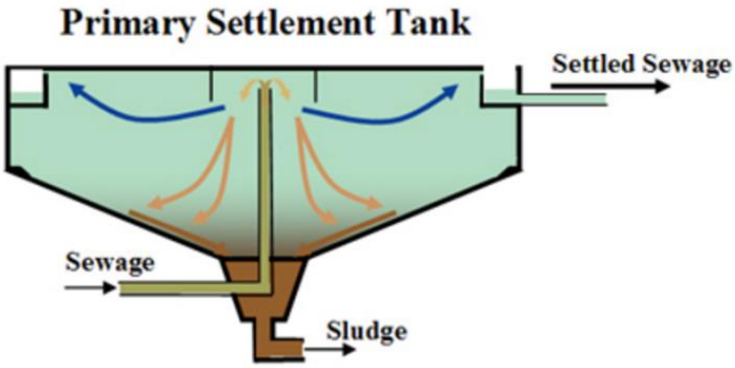


**Figure 3.** Primary sludge from gravitational settling [15].

The sludge material composition and TS content depend on the source of sludge. Table 2 shows the typical TS and some other characteristics of primary and secondary sludge. Because of the insignificant amount of tertiary sludge, this type is not considered here.

*Table 2. Municipal sludge characteristics* [16].

| Parameter | Primary | Secondary |
|---|---|---|
| Total solids (TS),% | 3.0–7.0 | 0.5–2.0 |
| Volatile solids (% of TS) | 60–80 | 50–60 |
| Nitrogen (N,% of TS) | 1.5–4.0 | 2.4–5.0 |
| Phosphorus ($P_2O_5$,% of TS) | 0.8–2.8 | 0.5–0.7 |
| Potash ($K_2O$,% TS) | 0–1.0 | 0.5–0.7 |

One important data about municipal sludge is its heat value based on the main sources of solid material from primary and secondary sludge (presented in Table 3).

*Table 3. Heat value in kJ/kg (kilo joule per kilogram) of primary and secondary sludge* [16].

| Heat Value of Municipal Sludge | | |
|---|---|---|
| Sludge type | Primary Sludge | Secondary Sludge |
| Heat Value (kJ/kg, dry basis) | 23,000 – 30,000 | 18,500 – 23,000 |

## 2.2 Mechanical Dewatering

Dewatering is the process of extracting water from a wet material or slurry via mechanical work. Water content, at any level of attachment to the solid part (free, floc, capillary, or bound water), is extracted without changing in phase from liquid to gas (water is in liquid form and separated in liquid form also). Changing phase is energy intensive and therefore expensive. Therefore, because it does not involve a change of phase, dewatering is relatively inexpensive from the energy consumption point of view. It is also relatively fast.

Mechanical dewatering is the first step in dehydration, and its results depend on the type of sludge (primary or secondary) and further options as the material content and its age (the older the sludge the lower level of TS after the dewatering and drying) as well as the type of dewatering machine. After dewatering, it is possible to have sludge cake with a TS content of up to 35% depending on the aforementioned factors [17]. A few dewatering systems advertise dewatering to 45%. [18]

Particle sizes of sewage sludge

The majority of dewatering machines perform solid liquid separation by taking advantage of filtration or screening. Therefore, to decide on the type of filter or screen, the first option is the particle size of the solid material inside the slurry. [19]

Sludge particle measurement is problematic, because of the wide size range of particles. Moreover, the sludge particle sizes are subject to change with digestion, treatment stage, and age (all of these factors make the particles smaller). [19]

Martinez and her colleges measured the size of sludge particles using a Beckmann Coulter LS 13 320 Laser Diffraction Particle Size Analyzer, a sophisticated and versatile device for particle size analysis. In their measurements, for each sample of sewage sludge, ten measurements were performed. The results are depicted in Figure 4 in terms of percentage or volume of particle regarding size range. [19]

There is at least one peak in Figure 4 for each graph that shows the mode of particle size. In other words, there is a range for each type of sludge that makes up the main portion of particle size. In all three graphs, the range from 5-300 µm (micrometer) is the major particle size. [19]

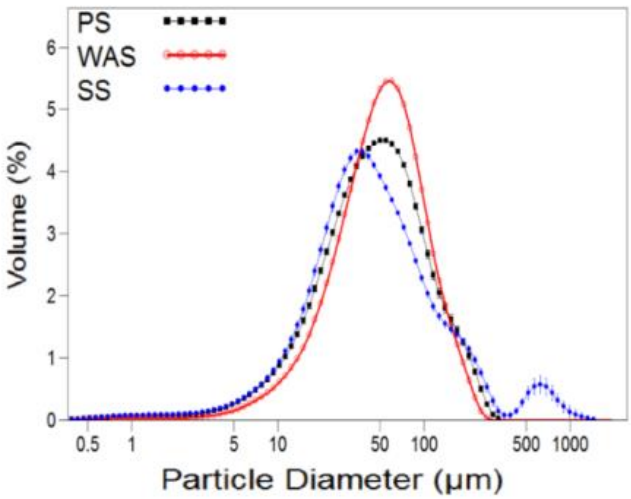


**Figure 4.** Particle size graph – PS stands for primary sludge, WAS is waste activated sludge or secondary sludge, and SS is the mixture of PS and WAS [19].

Table 4 shows mean values for the particle size and SSA (specific surface area) for all three types of sludge.

*Table 4. The mean value for the particle size and SSA* [19].

| Sludge Type | Size Average (µm) | SSA ($cm^2/mL$) |
|---|---|---|
| PS | 59.9 ± 2.90 | 2594 ± 129 |
| WAS | 61.0 ± 3.01 | 2672 ± 133 |
| SS | 65.9 ± 3.25 | 2031 ± 101 |

Particle size has a direct effect on water extraction. A smaller particle has a bigger SSA. Because of the bigger surface, the adhesion of water to smaller solid particles is stronger than its adhesion to bigger ones and makes the dehydration process more difficult. [19]

## 2.3 Effective factors in dewatering

Here four effective factors of, flocculants, air pressure effect, centrifugal function, and screening, that improve water extraction in dewatering process are presented.

### 2.3.1 Polymers (Flocculants)

To improve the water extraction efficiency of dewatering machines, synthetic polymers or flocculants are used for process conditioning [20]. Flocculants have large organic molecule configurations made up from long chains of monomer units with positive or negative electrical charge. A large number of monomer units make up each flocculent chain. These numbers are between a few thousands to millions of monomer units. These long and complex structures work like fishing nets to capture solid particles. In other words, they work as flocculants that chain solid particles together as shown in Figure 5 (left). Figure 5 (right) depicts the shape of a monomer unit and polymer chain. [21]

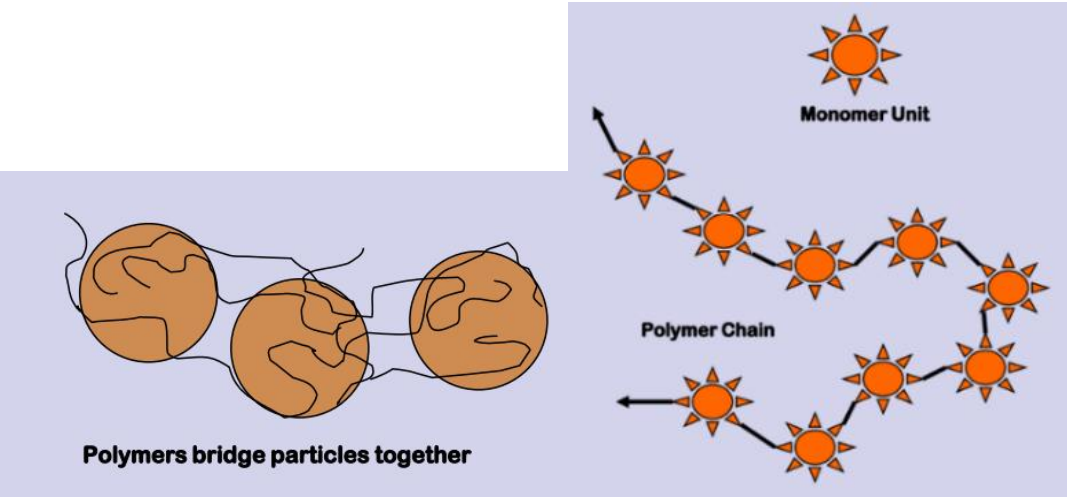


**Figure 5.** (left) Flocculants that chain solid particles together, (right) schematics of monomer unit and polymer chain [21].

### 2.3.2 Air pressure effect

Asmatulu conducted experiments to show the effect of air pressure-assisted centrifugal dewatering on galena, a natural mineral of lead sulfide. The best result was achieved at the highest air pressure and G force. In Table 5, the moisture contents at different air pressures and 2500 G are demonstrated. The average size of galena is smaller than 75µm, and the moisture content is about 18% before the dewatering process. This material is different from sewage sludge, and the dehydration of galena is easier. [22]

*Table 5. Results of dewatering using centrifugal force of 2500 G and air pressure ("None" value of air pressure is ambient pressure, other pressures are added pressures above atmospheric)* [22].

| Spin time (sec.) | Cake moisture (%) air pressure (kPa) | | | | |
|---|---|---|---|---|---|
| | None | 50 | 100 | 200 | 300 |
| 0 | 18.0 | 18.0 | 18.0 | 18.0 | 18.0 |
| 30 | 12.2 | 8.2 | 6.4 | 4.4 | 4.1 |
| 60 | 11.8 | 7.8 | 5.9 | 4.0 | 3.2 |
| 90 | 11.7 | 7.6 | 5.5 | 3.1 | 2.6 |
| 120 | 11.6 | 7.1 | 5.1 | 2.7 | 1.9 |

### 2.3.3 Centrifugal Function

Centrifugal dewatering is a process of separating solid materials from slurry by producing high centrifugal force. [22]

$$G = \frac{r\omega^2}{g} \tag{1}$$

The amount of the produced centrifugal force $G$ is calculated from Equation (1). Here, $r$ is radius of centrifugal vessel, $\omega$ is angular velocity, and $g$ is the earth's gravitational acceleration [22].

Darcy's law

Darcy's law is used to calculate the level of water extraction or flow rate through the sludge cake [22].

$$Q = \frac{K\Delta PA}{\mu L} \tag{2}$$

In Equation (2), $Q$ is flow rate, $K$ is the permeability of sludge cake, $\Delta P$ is pressure drop inside the sludge cake, $A$ is the surface of the filter area, $\mu$ is the dynamic viscosity of water, and $L$ is sludge cake thickness [22].

$$\Delta P = \frac{1}{2}\rho\omega^2(r_S^2 - r_0^2) \tag{3}$$

The pressure drop inside the sludge cake is calculated from Equation (3), which describes pressure drop during the filtration process [22]. In Equation (3), $\rho$ is water density, $r_S$ is radial distance from the sludge cake surface, and $r_0$ is the radial distance of free water (both $r_0$ and $r_S$ are measured from the rotational axis of the centrifuge) [22].

From Equation (3), the pressure difference across the sludge cake becomes zero when water disappears from the cake ($r_0$=$r_S$). If the water level decreases further, then $r_O$ will become greater than $r_S$, and the pressure inside the cake drops below atmospheric pressure. This may be the reason that pressure filters achieve a higher TS content than centrifuges for fine particles. [22]

Sludge cake has innumerable capillary vessels that trap water in the form of molecules and small water droplets. When the amount of water decreases, water droplets become smaller in size, the capillary pressure or surface attraction forces surpass the centrifugal force effect on the water particles. Therefore, the water extraction process will be stopped. In other

words, the centrifugal force works until the pressure applied is greater than the capillary pressure. [22]

$$P_p = \frac{2\gamma_{23} cos\theta}{r_p} \tag{4}$$

Equation (4) calculates capillary pressure $P_p$. Here, $r_p$ is capillary radius, $\gamma_{23}$ is surface tension, $\theta$ (as illustrated in Figure 6) is the angle between contact surfaces of solid-liquid-gas. Based on Equation (4), capillary pressure decreases with higher $\theta$ and $r$ along with lower $\gamma_{23}$. [22]

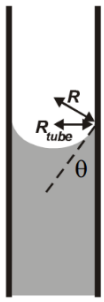


**Figure 6.** Contact surface angle of solid-liquid-gas [23].

### 2.3.4 Screening

Most dewatering systems use screens or filters to separate moisture from solid materials by producing a pressure difference across a boundary to force water through. For example, one side of screen is at higher pressure, while the other side is at lower pressure so moisture migrates to the lower-pressure area. In discussions regarding screening, moisture droplets can be considered very small particles. One purpose of screening is dewatering of wet and slurry materials. [24]

Screening is a common method for sizing and separating particles. The size range of materials in this field is from 300 mm to 40 µm, but efficiency diminishes by decreasing particle size. For screening smaller particles, a larger screen area is needed making the work expensive. [24]

The main criterion in screening efficiency is the displaced mass or recovery of the material's given size. Therefore, efficiency is calculated from the mass balance between two sides of the screen. Figure 7 shows the schematics of mass balance on a screen. [24]

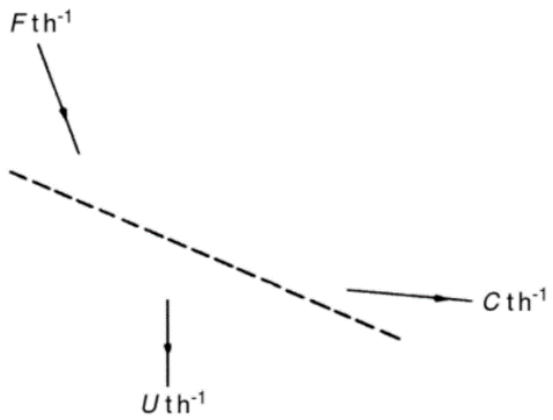


**Figure 7.** Mass balance of a screen [24].

In the figure, $F$th$^{-1}$ is the feed material, $U$th$^{-1}$ is the fine particles that pass through the screen, and $C$th$^{-1}$ is the coarse particles that flow over the screen [24].

$$E = \frac{(c - f_b)}{c(1 - f_b)} \tag{5}$$

The combined effectiveness or overall efficiency $E$ on a screen can be calculated from Equation (5). In this equation $f_b$ can be the amount of particles bigger than the screen apertures, and $c$ can be the portion in overflow. In practice, the amount of bigger particles in the underflow is assumed zero. In other words, the recovery of coarse material in the overflow is 100%. The path of particles bigger than the apertures is clear, but for smaller particles or particles roughly equal to the aperture size, the probability of passing through or overflowing depends on a few factors [24].

The first and the most important is their size and probability relationship. The probability of particles that are smaller and close the size of the apertures passing through the screen decreases tremendously when they are too close to the aperture size. [24]

Screen angle is the next factor: When the screen is at a shallow angle, the apertures aspect is smaller. Furthermore, angle affects the speed that materials are conveyed. Another factor is the screen's void fraction. There is a ratio between the area occupied by screen deck construction and the whole. A smaller void fraction passes less material. [24]

The last effective factor in screening is vibration. Screen vibration helps to both throw off particles from the holes and convey materials along the screen. If the screen vibrates

effectively, it will stratify the feed material as shown in Figure 8. Stratification forces smaller particles to move downward through other particles and towards the screen. Coarser particles move upwards to the top of the layer. The level of vibration should not be to low or high. Excessive vibration will bounce material from the screen surface. On the contrary, weak excitation cannot prevent screen holes from becoming plugged. [24]

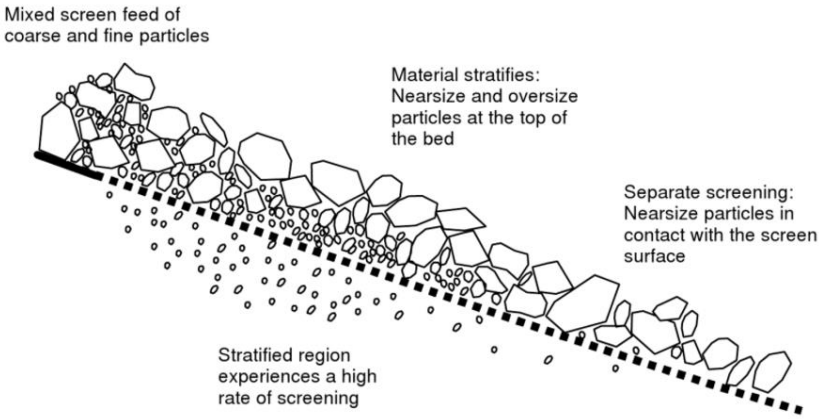


**Figure 8.** Stratification function [24].

$$\Gamma = \frac{a(2\pi f)^2}{9.81} \tag{6}$$

Equation (6) classifies the level of vibration by its intensity. Here, the vibration intensity is $\Gamma$, which depends on frequency $f$, and amplitude $a$. $2a$ (stroke) is referred to peak-to-peak amplitude. In general, for screens with big apertures, low frequencies and high amplitudes are more effective. For fine apertures, high frequencies and low amplitudes are more effective. The calculated intensity $\Gamma$ is a number multiplied by $G$. [24]

## 2.4 Oscillating screen with resonance phenomenon

Screen oscillation consumes a lot of energy, and much of this energy is wasted to continually change the direction of motion. Therefore, a screen oscillation system needs a powerful motor with eccentric drives or other oscillatory actuators. Screens that benefit from resonance phenomenon are good solutions for this issue. [24]

In these systems, the screen frame vibrates between rubber buffers and flexible hanger stripes. These restrict movement of screen (amplitude) and build up its connection to the dynamically balanced frame that has the same natural resonance frequency as the vibrating screen and three to four times more weight. Oscillatory motion, which drives on resonance

natural frequency of screen and frame, is translated from driver to the screen and stored in dynamically balanced frame and rubber buffers. Next, in the returning stroke, the stored energy is re-imparted to the screen, and it results in a lively sharp returning motion. Therefore, the wasted energy is minimal. The throw of dynamically balanced frame is less than the screen because of its heavier weight. Figure 9 shows rubber buffers and flexible hanger stripes making connection between a screen and a dynamically balanced frame. [24]

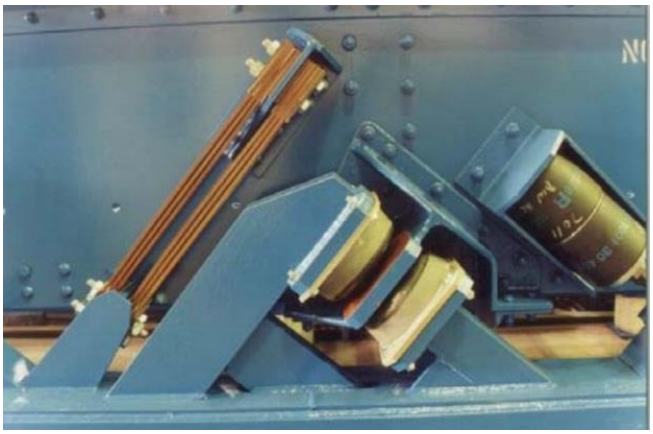

**Figure 9.** Rubber buffers and flexible hanger stripes [25].

### 2.4.1 Vibrating pattern generation

Vibrating screens mostly move in one of the circular, linear, or oval pattern motion [24]. Here some short descriptions about each of these patterns are presented.

*Circular motion, single shafts system:* In this pattern, the shaft of the inclined frame is located exactly at the center of gravity of the vibrating screen. The whole frame vibrates in a circular pattern as shown in Figure 10 (a). Another shape of motion is elliptical with circular oscillations at the ends and the middle of screen, respectively. See Figure 10 (b). This pattern is induced when the shaft is located above or below the center of gravity of the screen, at this condition the main axes of the oscillating ovals are towards the rotating shaft. [24]

The function sequence of the last pattern on processing materials is as follows. To begin, the oval motion of the feed head throws out the coarse particles forward to make the bed layer thinner. This work facilitates the discharge of the finest particles, which must be removed at one-third of the screen's length (in-flow vibration). Then, at the center of screen, circular motion slows down the material conveyance. Finally, near the outlet of screen, the vibration

makes the backward elliptical pattern that retains material longer for "near size particles" to have more time for extraction (contra-flow vibration). [24]

*Linear vibration, double shaft system:* This pattern is produced via a couple of matched unbalanced rotating shafts that rotate in opposite directions as shown in Figure 10 (c). The normal line to the distance center of the shafts makes the stroke angle to the screen surface. This angle is between 30° to 60°. The screen can be horizontal, upwards sloping, or downwards sloping. [24]

*Oval motion, triple shafts system:* Figure 10 (d) depicts a combination of three rotating unbalanced shafts. This horizontal assembly offers climbing elliptical vibration that has both linear vibration and tumbling effects on the processed material, which increases efficiency and process capacity over both circular and linear vibration machines. [24]

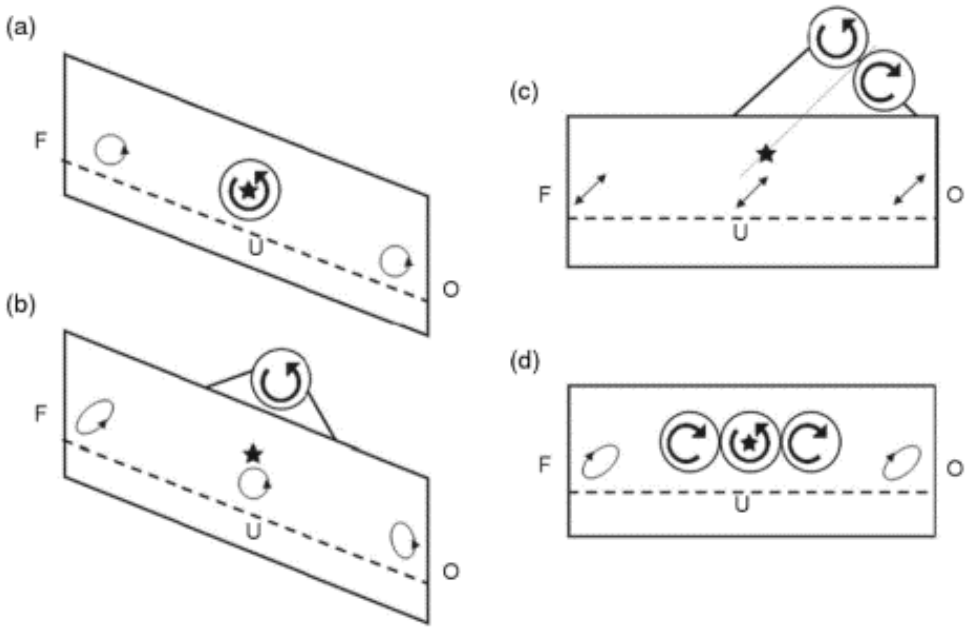


**Figure 10.** Different types of vibrating pattern – F indicates the feed or inlet end, O indicates the outlet, and the stars indicate the center of gravity [24].

## 2.5 Some sludge dewatering machines

This section presents some of the most common methods and machines used to dewater municipal sludge. Because it is difficult to transfer sludge with a total solids content greater than 25%, sludge dewatering to maximum dryness should be carried out in a continuous process. [18]

Centrifuge (Decanter)

The decanter centrifuge is one of the most common machines for sludge dewatering. Its energy consumption is not low, but the decanter has high productivity. The decanter relies on a high centrifugal force, normally between 2000 to 4000 G. This centrifugal force is applied directly on the feed sewage sludge and produces cake. The system works continuously, and flocculent materials should be fed constantly to be mixed with sludge to maintain dewatering efficiency. Centrifugal dewatering is like gravitational settling, it just benefits from centrifugal force to improve process time and efficiency. Figure 11 shows the typical configuration of a decanter centrifuge. [26]

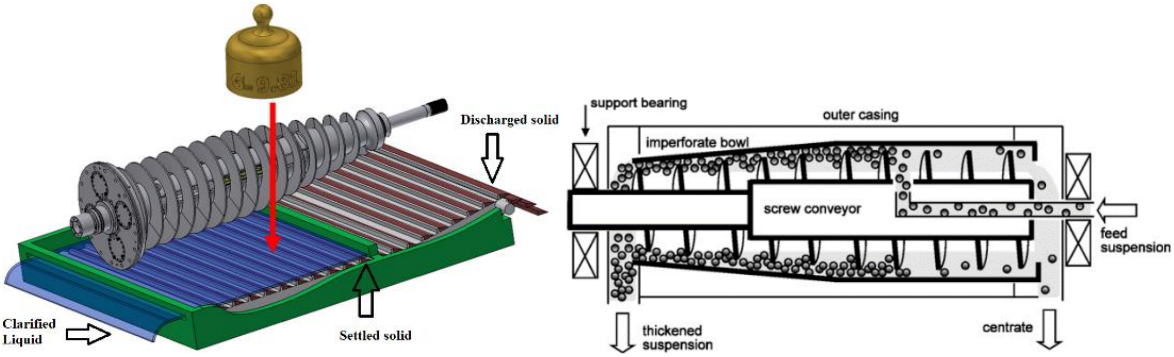


**Figure 11.** Schematic of decanter centrifuge [26,27].

In centrifugal systems, an over-torque problem can develop due to solids that accumulate inside the bowl. The screw is subjected to high wear by abrasive particles inside the sludge. [26]

Vibrating screen

The vibrating screen is a common system used for dewatering in the mining, environmental recycling, chemical, and food industries. The most important characteristics of these systems are their high capacity or throughput in addition to low operating cost and energy consumption. Furthermore, vibrating screens do not need flocculent. In these machines, the optimization of vibrating screen characteristics plays the fundamental and the most critical issue in their performance but practical tests are the normal guideline in this work instead of theoretical ones. [28]

Figure 12 shows a schematic of a vibration screen, the vibrational exciter in majority of cases is a crank driver, vibration motor, magnetic vibrator, or solenoid actuator. Here the

oscillatory motion of the screen acts as a conveyer that translates the material towards the outlet. [28]

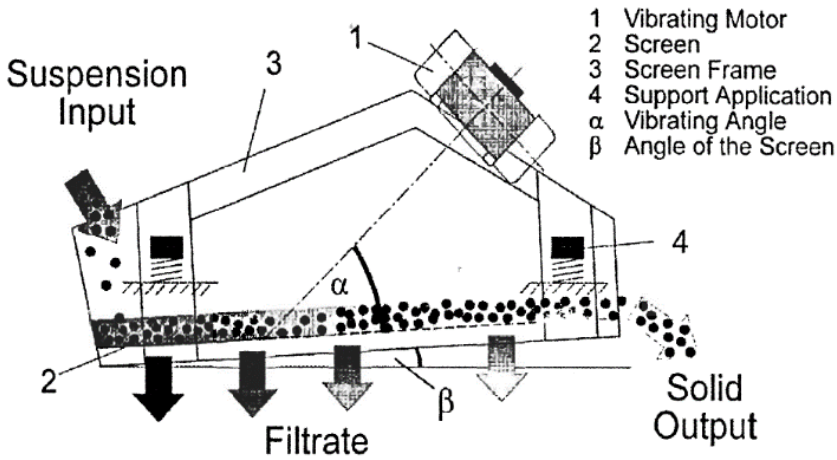


**Figure 12.** Schematic of a typical vibrating screen [28].

The machine has a simple structure, but deficiencies in the physical theory of vibrational dewatering makes up the main difficulty in designing vibration screens and analyzing the vibratory water extraction mechanism. The vibration frequency in these machines is normally between 30 - 60 Hz. [28]

The range of particle size for these systems is from 300 mm down to 45 µm that includes the range of sludge particle mean size values (from 57µm as lower range of PS to 69.15µm the upper range of SS) presented at "Particle sizes of sewage sludge". Aperture sizes and processed material particles define the capture rate of screen (bigger particles and smaller apertures result in higher capture rate and vice versa). [24]

A fundamental law in vibrating screens is that small particles need higher frequencies with lower amplitudes (as a role of thumb for particles down to 100µm of size, frequency about 60 Hz are implemented). Moreover, for materials with high moisture content, lower frequencies are more effective, and for lower moisture contents, higher frequencies work more practically. [24]

Rotary Press

In the rotary press, flocculate or polymer solution is injected at the inlet of the flocculator, and then is mixed with sludge in the flocculator unit. Flocculated sludge flows to the rotary

rectangular chamber of the press and rotates between two stainless steel chrome screen plates. Next, the high-pressure forces water through the rotational filter screens, and sludge is continually dewatered as the disk rotates inside the channel. Finally, the dewatered sludge forms a dewatered cake near the outlet. This machine works continuously. [18]

The level of dryness is adjusted via a gate that is rotated by a pneumatic actuator. By adjusting this system, the optimized level of dryness can be achieved. This machine works at a low speed of rotation. Therefore, it is a durable system with low maintenance expenses and energy consumption. [18]

Rotary press dewatering chamber is depicted in Figure 13. The lower curved arrow (A) shows the direction the restriction gate moves to decrease the level of TS. The upper arrow shows the rotational direction of the sludge inside the chamber. By narrowing the gate gap, the resulting TS will be increase. This dewatering system uses screen plates for solid-liquid separation. Fournier, one of the well-known rotary press producers, clams a capture rate for its machines of up to 95% (capture rate of the metallic screens). [29]

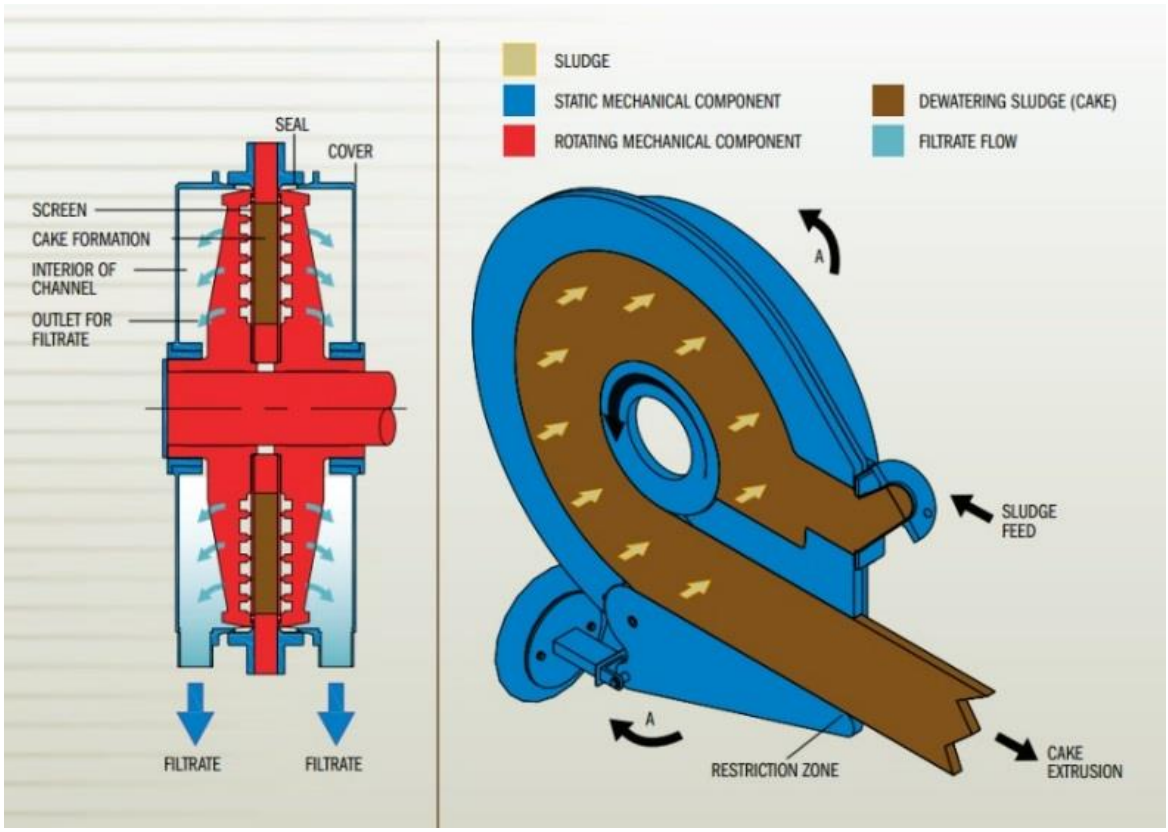


**Figure 13.** Rotary press [18].

Belt filter press

The belt filter press is another commonly used machine for sludge dewatering. This machine has two continuous filter cloths that are under constant tension. Flocculent is added to the sludge, which is then fed onto the lower cloth. The cloth works as both a pressure belt and conveyer. Primary dewatering starts under the influence of gravity when the belt carries sludge toward the consolidation zone where it is increasingly squeezed under the pressure from the upper belt. As it progresses, sludge volume is constricted. Simultaneously, the two belts pass over the rollers in a relative movement that induces shear stress on the sludge. As a result, the sludge is not only compressed between the rollers, but it also is subjected to shear. The combined mechanisms produce dryer cake. [26]

Flocculate must be added to the sludge for this machine to operate effectively and to avoid accumulation of solid particles inside the filter belt. Moreover, flocculent facilitates the gravitational drainage of the sludge during the primary section of dewatering. [26]

The belts must be washed prior to the return cycle, and the water flow should be between 50 to 200% of the feed sludge. The feed sludge is recommended to have 3-4% of TS. Figure 14 shows typical belt filter press. [26]

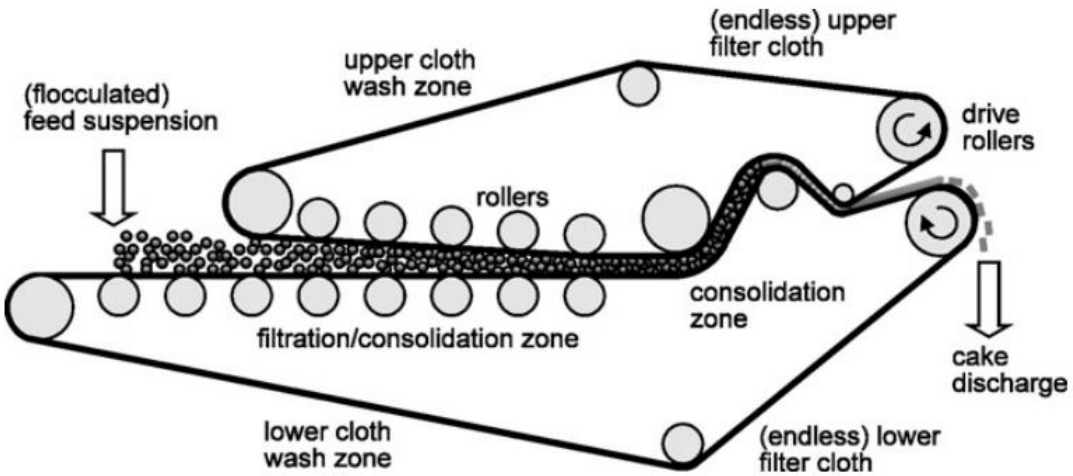


**Figure 14.** Schematic of a belt filter press [26].

Filter press

The filter press is another common machine for sludge dewatering. It uses from 60 to 80 filter plates of about 1.5 m*1.5 m or 2 m*2 m recently, bigger plates are becoming more common. [26]

In sequence, the filter-press dewatering cycle is as follows. First, flocculated sludge is fed into the machine. Then, the membrane cake is press squeezed to extract water. Next, air is blown through the cake. Finally, the trapped particles are washed or blown out from the filter plates. Figure 15 (left) illustrates the filter press membranes. In some of the new systems to improve the dewatering performance and have more uniform water extraction after the pressurization step, sludge is compressed under pressure by a diaphragm that is pressurized up to 16 bar. See Figure 15 (right). [26]

A big weakness of this machine is that the filter cloths must be washed frequently to maintain the efficiency of water extraction. The system does not work continuously, however many of steps are now automated. [26]

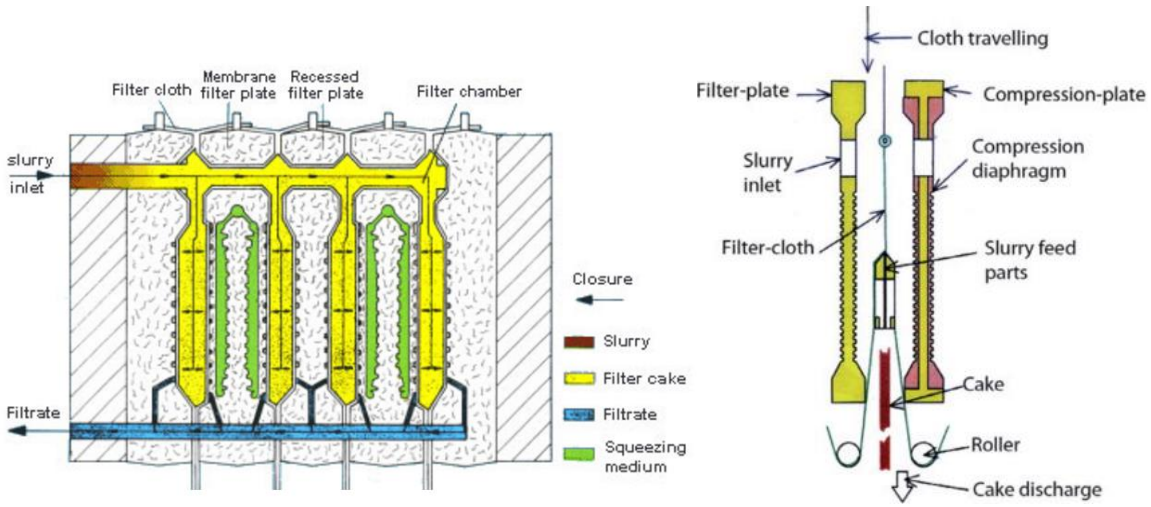


**Figure 15.** (left) Schematic of filter press membranes [30]; (right) the mechanism of pneumatic compression diaphragm [31].

Rotary vacuum drum filters

Rotary vacuum drum filters work continuously, and they are operated automatically. However, they have some challenging filter-type limitations for municipal sludge dewatering. The level of vacuum applied to the system defines the driving force of the dewatering. Based on practical experience, a vacuum level of more than a quarter of bar (0.25 bar) is not used for these machines, which restricts the system to particle sizes smaller than 2 µm. [26]

Rotary vacuum drum filters are more suitable for industrial sludge dewatering [26]. Figure 16 shows the schematic of a rotary vacuum drum filter.

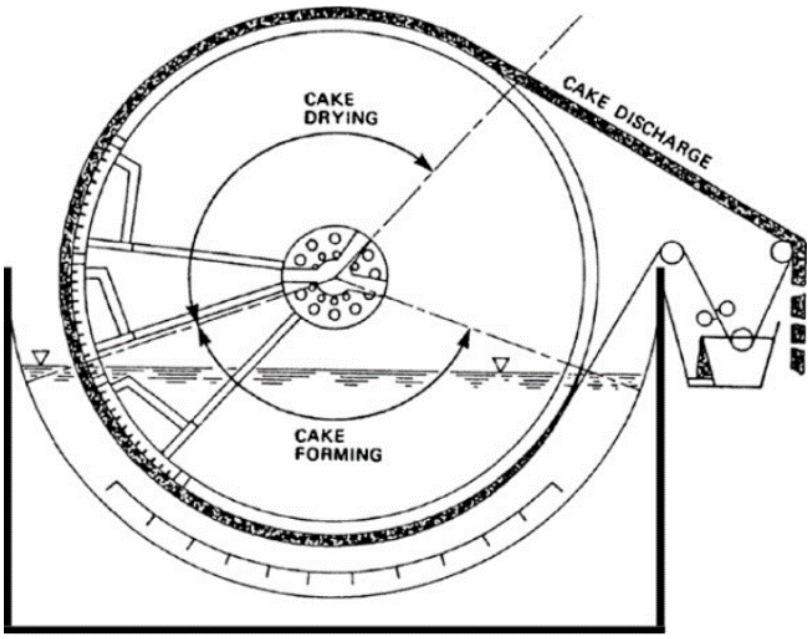


**Figure 16.** Diagram of rotary vacuum drum filter [26].

Other dewatering systems that are not described here are either not commonly used for municipal wastewater sludge dewatering or have weaknesses. For example, among centrifugal machines, on the decanter is applied to municipal sludge dewatering. The screw press is suited to the dewatering of fibrous sludge. EKG dewatering bags are effective, but demand large areas of land, which makes their application cost prohibitive. Additionally, the EKD dewatering method is slow and time-consuming. [32]

## 2.6 Dewatering energy consumption

To produce tangible data in the form of kilowatt-hours (kWh) and euros for some different dewatering machines, their energy consumptions in kWh were evaluated based on their productivity and then translated into euro. In Finland the price of electricity in the year 2014 was 0.072 €/kWh [33].

The density of sludge depends on material content, but it is on average about 1000 kilograms per cubic meter ($kg/m^3$) [32]. Table 6 shows the result of energy consumption and price for some dewatering systems in relation to their capacity.

*Table 6. Energy consumption and price for four dewatering machines illustrating price for increasing the level of dryness by 10% more* [32].

| Dewatering machine | Energy consumption (kWh/ton/10% increase in TS) | Price (€/ton/10% increase in TS) |
|---|---|---|
| Rotary press | 0,083 | 0,006 |
| Centrifuge (decanter) | 0,583 | 0,042 |
| Belt filter press | 0,111 | 0,008 |
| Filter press | 0,125 | 0,009 |

The dewatering process is more economical from the energy consumption point of view. Furthermore, it is a faster process that extracts a large percentage of water content in a short period.

## 2.7 Drying

If a higher solids content than is available from dewatering is needed to support efficient incineration or to decrease transportation cost in a disposal solution, a drying solution will be needed.

### Theory of boiling, vaporization, and sublimation

Water ($H_2O$) can exists in three commonly known states: solid, liquid, and gas. It can also exist as a plasma, a fourth state. When heat is added, the temperature of the solid, liquid, or gaseous states increases linearly. However, as water changes phase, its temperature remains constant and all the energy input is used to overcome the latent heat of the phase change. A large amount of energy must be input to change the phase of water from liquid to vapor.

For water six processes of change in phase are classified that are listed below with the amount of specific absorbed (-) or released (+) latent heat [34]:

Melting: water state changed from solid to liquid, -330 kJ/kg

Evaporation: water state changed from liquid to gas, -2,500 kJ/kg

Sublimation: water state changed from solid to gas, -2.830 kJ/kg

Freezing: water state changed from liquid to solid, +330 kJ/kg

Condensation: water state changed from gas to liquid, +2,500 kJ/kg

Disposition: water state changed from gas to solid, +2,830 kJ/kg

For drying purposes, the moisture content must be vaporized or sublimated. Both evaporation and sublimation (freeze-drying) demand a lot of energy. [34]

Figure 17 nicely illustrates the latent heat or enthalpy of water at different states. In this graph, the unit of energy is kilocalories per mole (kcal/mol). If the units were anything else, the shape of graph would not be changed. As depicted in the picture, the highest amount of energy is consumed in changing the phase from liquid to gas. The amount of required heat energy for vaporization is roughly 6 times that of boiling from 0°C to 100°C. [34]

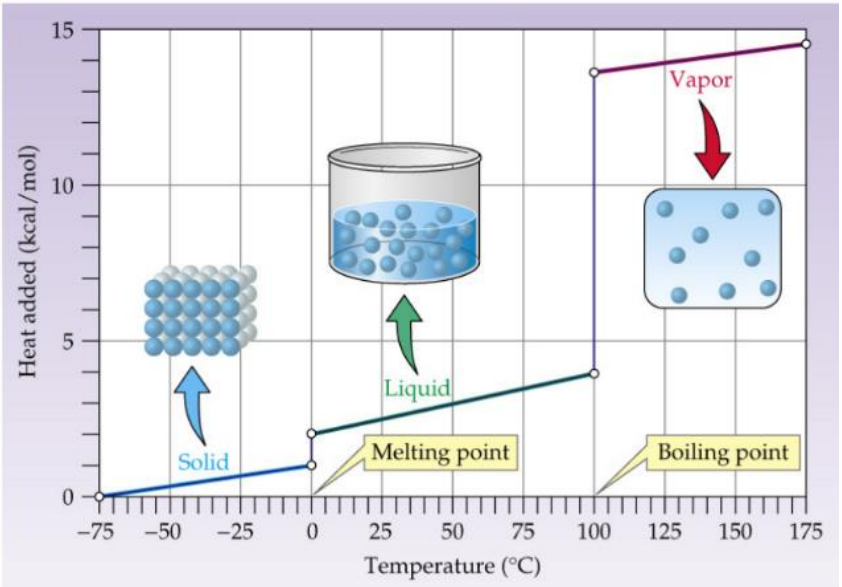


**Figure 17.** An illustration of latent heat or enthalpy of water at different states [35].

## 2.8 Thermal energy consumption under vacuum

To increase the drying rate or perform the evaporation process in a shorter period, one effective way is to apply vacuum. Water can be boiled at any temperature if the pressure it is subjected to is properly regulated. [36]

A surface phenomenon, evaporation takes place when water molecules have enough kinetic energy to escape from the liquid surface. Because at higher temperatures the kinetic energy of molecules is greater, the evaporation rate is higher. To reach that level of kinetic energy those molecules that are beginning to escape, absorb heat energy (large amount of heat of vaporization) from their surrounding area. [36]

The evaporation phenomenon can continue in a closed container until the number of escaping molecules equals the molecules entering the liquid or condensing back into it. At this condition, the atmosphere of the container is saturated, or in other words, vapor reaches the saturation vapor pressure. [36]

The boiling point is the temperature at which the saturated vapor pressure of the liquid is equal to its atmospheric pressure. In water, the saturated vapor pressure is 100°C at sea level. The pressure is 760 mmHg, 760 torr, or 1 atmosphere. The vapor pressure increases and decreases with temperature. Therefore, if the pressure decreases, the boiling temperature will also decrease. It is possible to boil water at ambient temperature in a vacuum. In Figure 18, the approximate boiling points corresponding to higher and lower sea level pressures are depicted. [36]

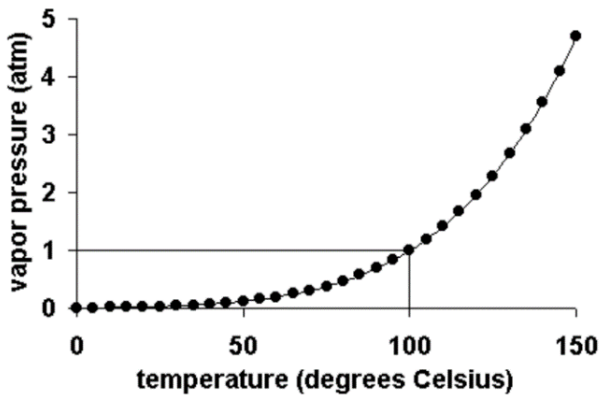


**Figure 18.** Boiling temperature and pressure graph [37].

When pressure decreases, water evaporates at temperatures below 100°C, but it still needs the enthalpy of vaporization. Based on Figure 19, the amount of enthalpy of vaporization at lower pressure is higher than the enthalpy at higher pressure. Therefore, when the water is boiled and vaporized at lower pressure, some energy is saved, because there is no need to add heat for boiling, and the water can start boiling at ambient temperature. On the other hand, it needs more energy for vaporization. [38]

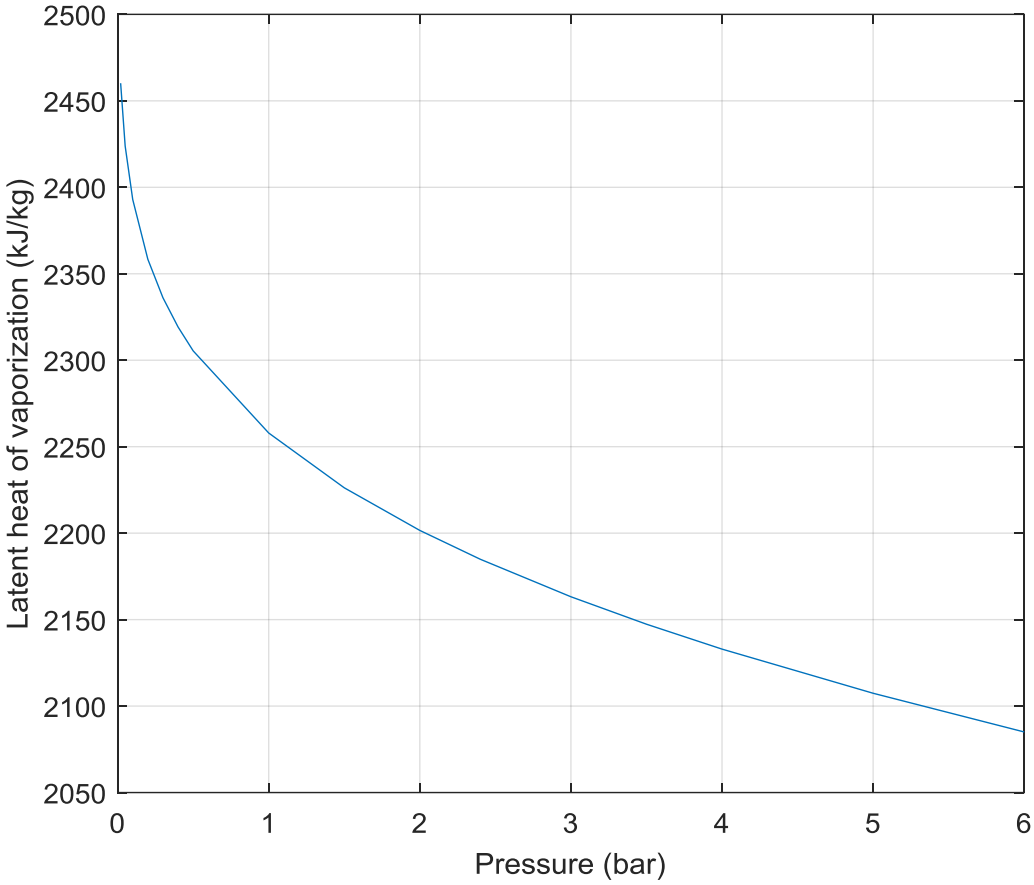


**Figure 19.** Enthalpy of vaporization for water under different pressures from 0.02 to 6 bar.

### 2.8.1 Comparison of vaporization energy requirement with and without vacuum

The process to change the phase of one kilogram of free water from 0°C in liquid state to gas can be performed in two scenarios. One way is to increase its temperature to 100°C, and then go from boiling water to gas, which has the same temperature. Another method is to make vacuum and boil water at the ambient or lower temperatures then give it enough energy to change its phase. For comparison, two pressures, 1 and 0.2 bar, are selected.

*First scenario (at 1 bar pressure)*

Water starts boiling at 99.63°C under 1 bar of absolute pressure. The amount of heat to increase the temperature from 0°C to 99.63°C is 417.51 kJ/kg. Now, water needs the enthalpy of vaporization to change its phase from liquid to gas, which is about 2257.92 kJ/kg at 99.63°C [39]. Therefore, the total amount of heat energy is 2675.43 kJ/kg. At 99.63°C and 1 bar of absolute pressure the specific volume of water vapor is about 1629 times more than liquid water at the same condition [38,39].

*Second scenario (under vacuum of 0.02 bar)*

Water starts boiling at 17.51°C under 0.02 bar of absolute pressure. The amount of heat to increase the temperature from 0°C to 17.51°C is 73.45 kJ/kg. Now, water needs the enthalpy of vaporization to change its phase from liquid to gas, which is about 2460.19 kJ/kg at 17.51°C [39]. Therefore, the total amount of heat energy is 2533.64 kJ/kg. At 17.51°C and 0.02 bar of absolute pressure the specific volume of water vapor is about 67006 times more than liquid water at the same condition [38,39].

The difference between the total energy consumption between vaporization at 0.02 and 1 bar is 141.79 kJ/kg. That is about 5% conservation in the total heat energy consumption of atmospheric vaporization. However, using vacuum increases the rate of drying speed significantly. Moreover, it lowers the temperature requirement, making it possible to drive the process using less expensive energy such as waste heat.

If the latent heat of vaporization is not added to the water under the vacuum condition, the water will freeze and will not evaporate, because in vacuum water starts to boil and a small portion of it will be vaporized. For vaporization, it takes the enthalpy of vaporization from the surrounding area. Therefore, the water content of the material starts to be frozen. This makes up the fundamental idea of freeze-drying. Next, the heat of sublimation is gradually fed into it (normally in the span time of 24 hours). This method of slowly heating saves the shape of material. In freeze-drying, the moisture content that is in the form of ice will be sublimated.

Vacuum drying effectively improves drying kinetics. Therefore, one possibility for an economical drying process could to use lower temperature and vacuum to maintain drying kinetics.

If the vacuum drying system of the sludge processing is located near the furnace and sludge burning facilities then it could be possible to use from the waste heat of the furnace as the heat input for the vacuum drier, then this free source of energy can be used as the latent heat of vaporization for sludge water content.

## 2.9 Commercially available sludge dryers

There are three modes of heat transfer. *Conduction* is the energy transfer from particle to particle. *Convection* is the transfer of heat by the motion of high energy or hot matter, this method happens by the translation of gases or liquids like vapor or hot flow current. *Radiation* is the translation of heat energy via electromagnetic waves like sunlight. Drying machines that dry materials like sludge work based on one or some of the mentioned heat transfer principles. Here some of the most common methods and machines for municipal sludge drying are presented.

### Solar drying

Since the thermal drying process is known as a very energy intensive process, the first natural method for drying sludge is solar energy that is free, green, and sustainable. Solar sludge drying works based on horticultural greenhouse with venting and stirring systems. [16]

Solar energy can be collected using asphalt or clay-lined beds. The asphalt beds are more effective. Continually churning the sludge makes the process faster, decreases odor, and reduces the gathering of insects. If the sludge is not churned, it develops a dry surface layer that inhibits the drying process. [16]

In warm locations, solar collectors can efficiently dry sludge at a short period. However, in cold places, these facilities are useless or have a minimal productivity. Figure 20 shows a schematic of a greenhouse closed solar sludge dryer. Here, the dewatered sludge enters the greenhouse from the intake side. Then, the rotary scarifier breaks the sludge into small granules, gradually pushing it toward the exit. To prevent moisture saturation from inhibiting the vaporization process, a ventilation system continuously evacuates moist air. [16]

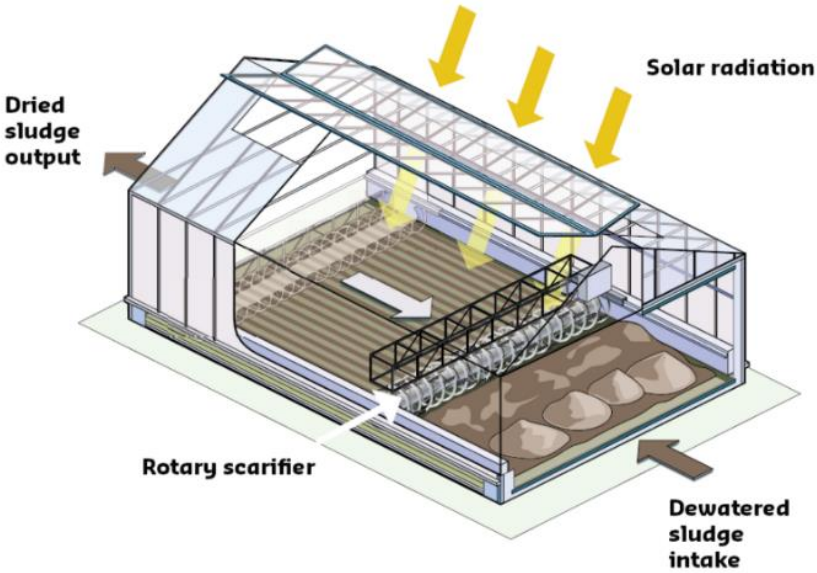


**Figure 20.** Solar greenhouse dryer [40].

Thermal drying

Solar drying demands wide land area, another issue is its odor problem, so recently in many countries, the focus has shifted to thermal drying as a main sludge drying technology. According to heat temperature and mass transfer, drying methods can be divided into three main categories: direct, indirect, and combined drying systems. The final TS and the drying kinetics of the sludge are to a high degree depended on sludge type and the drying method. Therefore, for each drying system the type of sludge defines its drying kinetics curve. Figure 21 shows the drying kinetics curve of PS, WAS, and SS. As depicted, PS is the most favorite sludge for drying and WAS the most expensive. [16]

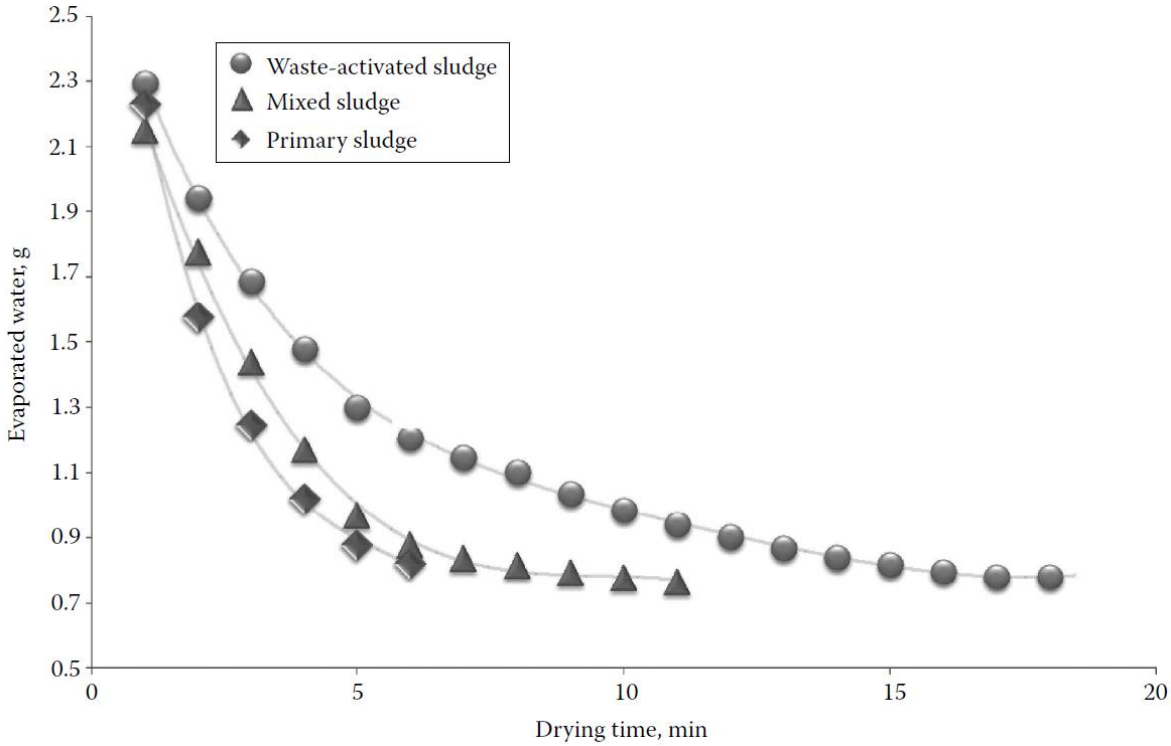


**Figure 21.** Drying profiles of primary (PS), activated (WAS), and mixed sludge (SS) [modified, 16].

Based on the type of drying machine and sludge, a TS content of up to 95% can be achieved. Some companies clam their machines can dry sludge up to 99%. Some typical thermal sludge dryers are presented in the following paragraphs. [16]

Direct (convection) drying

*Rotary dryers*, depending on their design offer differences in productivity and efficiency and operate at differing inlet temperatures. The normal inlet temperature in these systems is up to 1000°C, and the range of water evaporation rate is from 800-50,000 kg/h. Figure 22 shows a typical mechanism of a rotary dryer. [16]

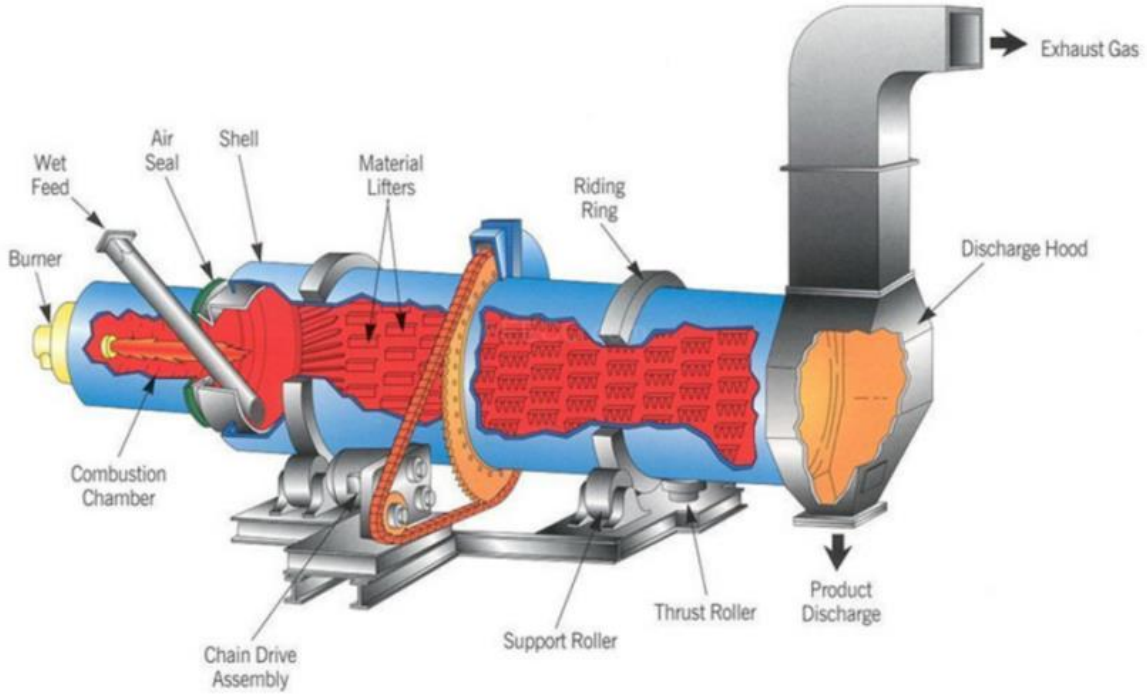


**Figure 22.** Rotary dryer [41].

*Flash dryers* agitate feed sludge using a cage mill to increase turbulence and expose sludge to hot air. The rotation of the rotor pushes the partially dried particles up where they will be dried more. Dried particles return to the bottom to mix with incoming feed sludge. In this machine, the highest amount of evaporated water in the airflow is about 0.1 kg/m$^3$ at the vent fan. The water evaporation rate of a flash dryer depends on particle size, which is something between 5-100 kg/h. Figure 23 shows a schematic of a flash dryer. [16]

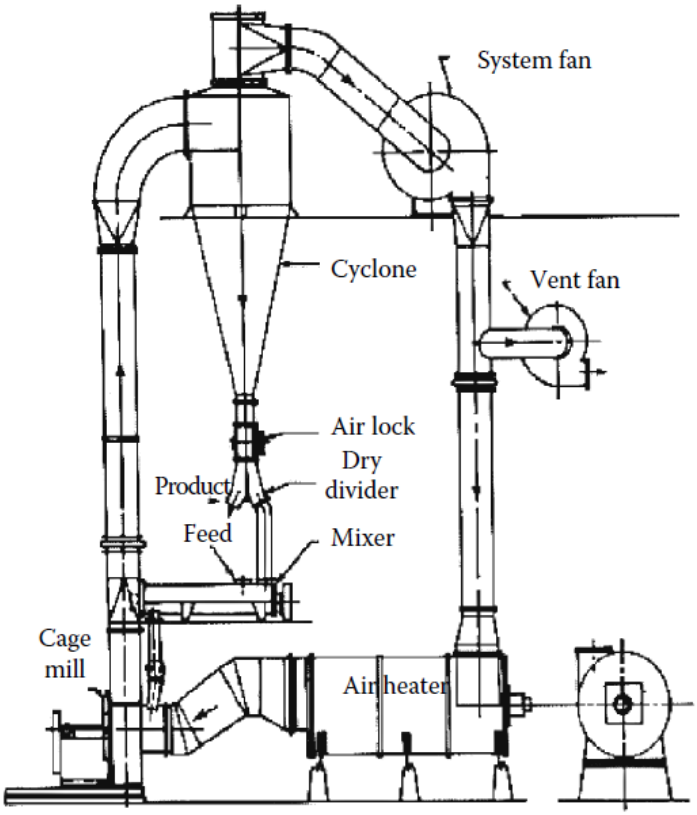


**Figure 23.** Flash dryer [16].

Indirect (conduction) drying

The heat transfer method in indirect dryers is via hot internal surfaces of the machine. As there is not any direct contact with the flame, the working temperature is lower than the direct drying systems. [16]

*Paddle dryers* agitate sludge, while protecting machine parts and surfaces from sludge accumulation. When it is at about 55-70% TS, sludge is particularly sticky. Figure 24 shows a paddle-drying machine and a paddle blade. [16]

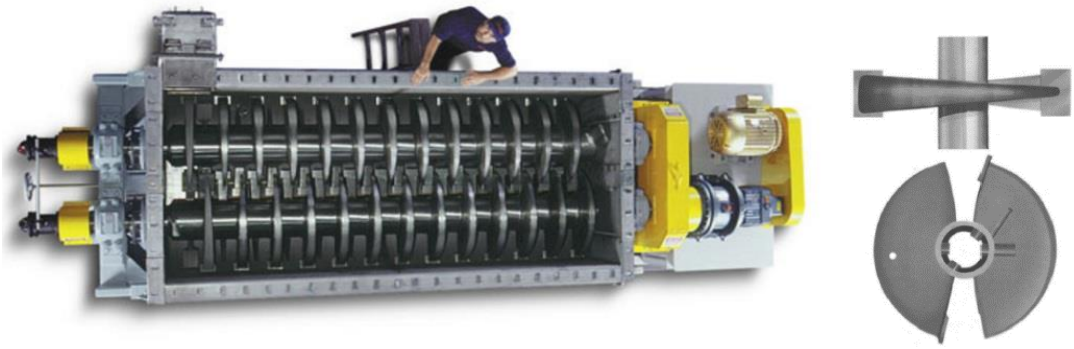

**Figure 24.** A paddle-drying machine (left) [42], and a paddle blade (right) [16].

Other drying methods

Besides dryers working based on conduction or convection, other dryers are available that use a combination of conduction and convection or other methods [16].

*Fluidized bed dryers* - Moving sludge inside a fluidized bed dryer is done with few mechanical parts. The heat of vaporization is supplied from the pipes that carry hot oil. Figure 25 shows a schematic of fluidized bed dryer with heating tubes. [16]

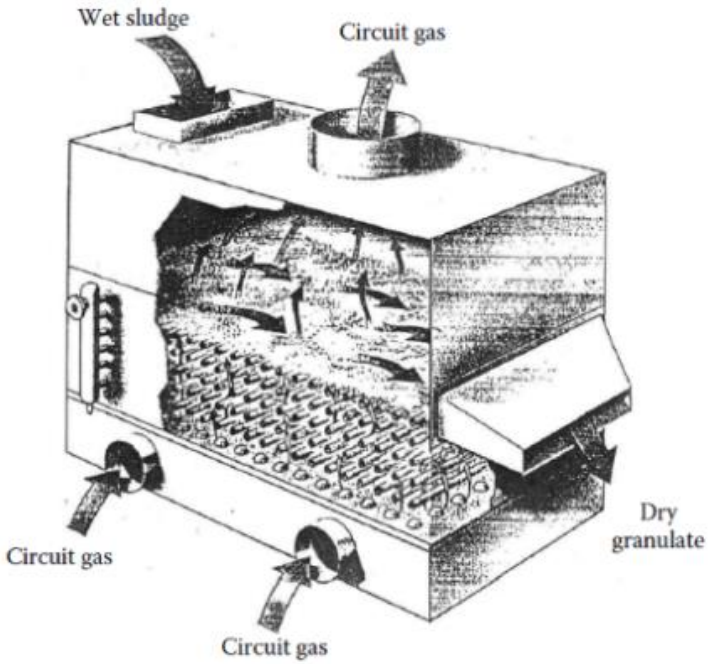


**Figure 25.** Schematic of fluidized bed dryer [16].

## 2.10 Drying energy consumption

Table 7 represents the energy consumption values of four thermal drying machines. The presented numbers are approximate and are greatly depended on the design (brand) and the efficiency of the related machine. [16]

*Table 7. Some sludge dryer energy consumptions* [16,43].

| Drying machine | Energy consumption (kJ/kg for evaporated water) |
|---|---|
| Rotary dryer | 4,600-9,200 |
| Flash dryer | 4,500-9,000 |
| Paddle dryer | About 5,600 |
| Fluidized bed dryer | 4,000-6,000 |

Just for a comparison, entropy of vaporization (for free water) is about 2600 kJ/kg, but the energy consumptions to vaporize one kilogram of water in the mentioned drying machines are higher. This big difference is mostly because of the mixed water in sludge in the form of capillary or bound water. [16]

The source of heat energy in drying machines can be biogas from digestion reactors, natural gas, or geothermal energy that does not have the same price [16].

## 2.11 Energy consumption comparison between dewatering and drying

At the beginning of the PAKU project, based on a comparison that conducted between some different dewatering and drying machines, it was evaluated that energy consumption for drying process on average is about 300 times more expensive than dewatering [32]. The price for drying is 6.2 € and dewatering 0.02 € for each ton of sludge to increase its TS by 10% [32]. In another research, it came out that drying is 100 to 500 times more expensive than dewatering that supports PAKU result [43].

# 3 THEORY OF HIGH FREQUENCY VIBRATION

Ultrasonic dewatering is a new method for water extraction that mostly is under investigation in laboratory scale and recently has been used in few industries for dewatering.

Part of understanding assisted dehydration using high power ultrasound is the study of vibrational translation inside the field of materials. Therefore, this section is to become familiar with the terminology of ultrasound. The main characteristics of ultrasound is similar to sound, the only thing that divided them into two separate areas is the human hearing ability, man can roughly hear frequencies from 20 Hz to 20 kHz and any frequency above 20 kHz is called ultrasound. [44]

## 3.1 Theory of sound

Sound is a sequence of compressions and rarefactions inside a material that could be gas, liquid, or solid. Therefore, sound is only vibration that is translated inside a media and the method that men sense it is via their ears and interprets as sound, so maybe it is better to call it vibration translation or sorts of compressed and rarefied molecules. [44]

### Velocity of sound

The velocity of sound in air is a function of air temperature. It increases with increasing air temperature and vice versa. [45]

$$v_{air} = 331\left(\frac{T}{273}\right)^{\frac{1}{2}} \tag{7}$$

In Equation (7), $v_{air}$ is the velocity of sound in air, $T$ is temperature in degrees of kelvin, and 331 m/s is the speed of sound at 0°C (273 °k) in air [45].

At high altitude, where the temperature is about -50°C, commercial airplanes should fly slower than the sound speed near the surface. At 20°C, the speed of sound is about 343 m/s. At -50°C, it is about 299 m/s, so there is a high risk of sonic boom, and dangerous vibrations can damage the structure of the flying machine.

In addition, the speed of sound is depended on bulk modulus and density of the translating media [45].

$$v = (\frac{B}{\rho})^{\frac{1}{2}} \tag{8}$$

In Equation (8), $v$ is the speed of sound in a predefined media, $B$ is bulk modulus of the media, and $\rho$ is the density of the media that sound is propagating inside of it [45].

Because the ratio of bulk modulus to density of water is bigger than the air and respectively in steel this ratio is still bigger than water. The speed of sound increases in these materials.

### 3.1.1 Sound intensity

Sound intensity is the power of sound per unit area. [45]

$$I = \frac{P}{A}[\mathrm{W/m2}] \tag{9}$$

In Equation (9), $P$ is power in watt, $A$ is area in $m^2$, and $I$ is intensity in watt per square meter ($W/m^2$). [45]

The threshold of hearing for a human is $1*10^{-12}$ $W/m^2$, and the intensity of a normal speech is about $1*10^{-6}$ $W/m^2$. The threshold of pain for man (*i.e.*, the maximum tolerable sound intensity) is about 1 $W/m^2$, which is something like standing near the runway of an airport when an airplane with a jet engine takes off at full thrust. [45]

Decibel scale

Representing intensity in $W/m^2$ results in large numbers, so a base 10 logarithmic scale is used to represent sound in decibels. Decibels are defined with respect to human hearing capability. In a decibel scale, $1*10^{-12}$ $W/m^2$, threshold of hearing, is the denominator and the subjected intensity for conversion is the nominator of ratio. [45]

$$I(dB) = 10\log(\frac{I}{I_0}) \tag{10}$$

In Equation (10), $I_0$ is the threshold of hearing, and $I(dB)$ is the intensity in decibel [45]. Therefore, the threshold of hearing in decibel scale is zero, and the threshold of pain is 120 dB. When the sound source is doubled, the intensity in $W/m^2$ doubles, but intensity in dB just increases 3 dB. So, if the source becomes four times greater, 6 dB will be added into its dB scale. Respectively, if sound source increases by the factor of 10 (10 times bigger) in dB scale intensity will increase 10 dB.

### 3.1.2 Effect of distance on sound intensity

The intensity of sound is proportional to the reversed ratio of the distance squared, respectively. Energy intensity of sound is spread over a spherical surface. [46]

$$I = \frac{P}{4\pi R^2} = \frac{P}{A_s} \tag{11}$$

In Equation (11), $R$ is for distance from the sound source, and $A_s$ is surface area of sphere [46].

By the last equation, the intensity at any distance from the source can be found when the amount of source power is known. In this equation damping is not considered. Therefore, if any user wants to use sound vibrational energy, it will be crucial to avoid big gaps between vibrator and energy consumer. Figure 26 shows the surface increase because of distance from the source.

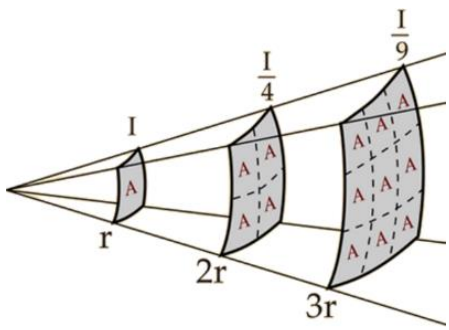


**Figure 26.** Surface increase because of distance from source [47].

### 3.1.3 Intensity of sound and wave characteristics

$$I = \frac{P}{A} = \frac{1}{2}\rho v f^2 S^2 \tag{12}$$

Equation (12) shows the relation of propagating wave properties and intensity.

Besides the source power according to this equation, intensity is related to media density ($\rho$), wave propagation speed ($v$), frequency ($f$), and the particle displacement or wave amplitude ($S$) [46].

In sludge, the speed of sound and the density are not under control, but it is possible to manipulate frequency and the amplitude of the vibration to change the intensity [46].

Interference of waves

Coherent waves are two or more waves that not only have the same frequency but also leave the source at the same time. When there are two coherent sources of sound or vibration, by

managing the distance from the sources, based on their phase difference, one audience can hear constructive interference of sound that is 3 dB louder than any of the sources or destructive interference that the audience will hear nothing. Figure 27 shows these interferences. [46]

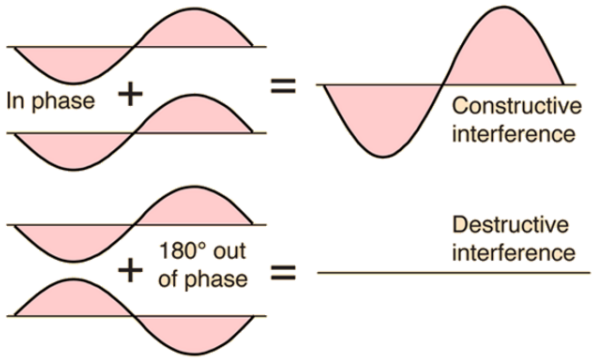


**Figure 27.** Constructive and destructive interferences [44].

## 3.2 Standing waves

The method of energy propagation in ultrasonic processes is via standing waves, because no material is translated. Standing waves can be regarded as the superposition of two waves that are moving towards each other and added together.

When a wave enters from one media into another, one characteristic that will be changed is the wave speed. Because of this change in speed, part of the wave will penetrate into the second media, and a portion of it will be reflected. The higher the wave speed difference is in each of the two media, the greater the portion of the wave that is reflected will be. The wave propagation speed is the same as the description of the speed of sound and is determined by the material characteristics and conditions like temperature and pressure. In the case of wave or energy absorption, the absorbed wave produces heat. [48]

Vibration modes in any media, as a string under tension, air, water, or sludge, have identical or characteristic shapes (mode shapes) in the form of standing waves or resultants which are constructed from the incident and reflected waves and vibrate in their resonance harmonic motions (they are associated with resonance frequencies). An incident wave will be reflected with 180° change in phase if the support is fixed (wall). [48] The situation of incident, reflected, and resultant waves are illustrated in Figure 28.

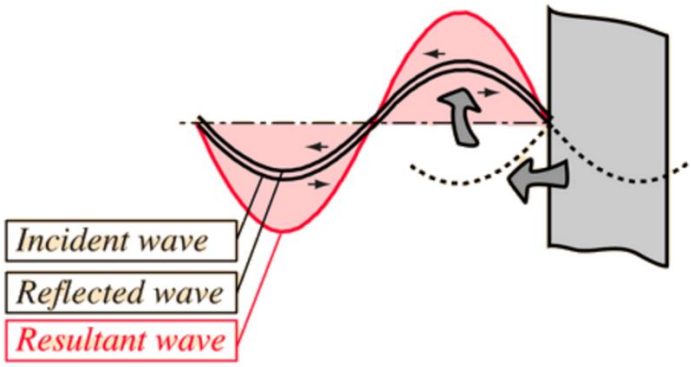


**Figure 28.** Incident, reflected, and created standing waves [modified, 44].

In standing waves, the media vibrates only in some regions (antinodes), and it is fixed in others (nodes) [49]. Figure 29 shows nodes and antinodes.

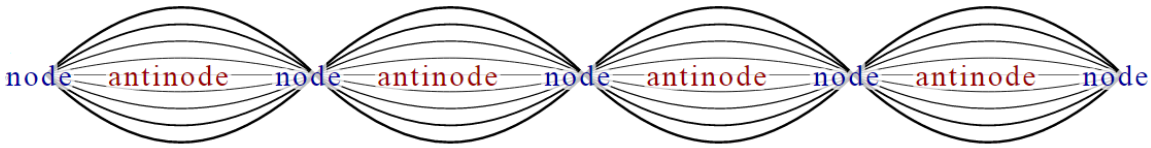


**Figure 29.** Location of nodes and antinodes in a field of material like a string [49].

## 3.3 Pressure wave osculation

Besides displacement, the important characteristic of standing waves in this study is pressure. As depicted in Figure 30, at the points of maximum displacement (the antinodes) in an air column, there is no change in pressure. And, at zero displacements (the nodes), the highest alternating pressures are produced. The pressure level of pressure nodes is the mean value of the highest and lowest pressure (more elaboration in the Figure 30). Therefore, the nodes of pressure are the antinodes of displacements and vice versa. There is 90° phase shift between pressure and displacement. [44]

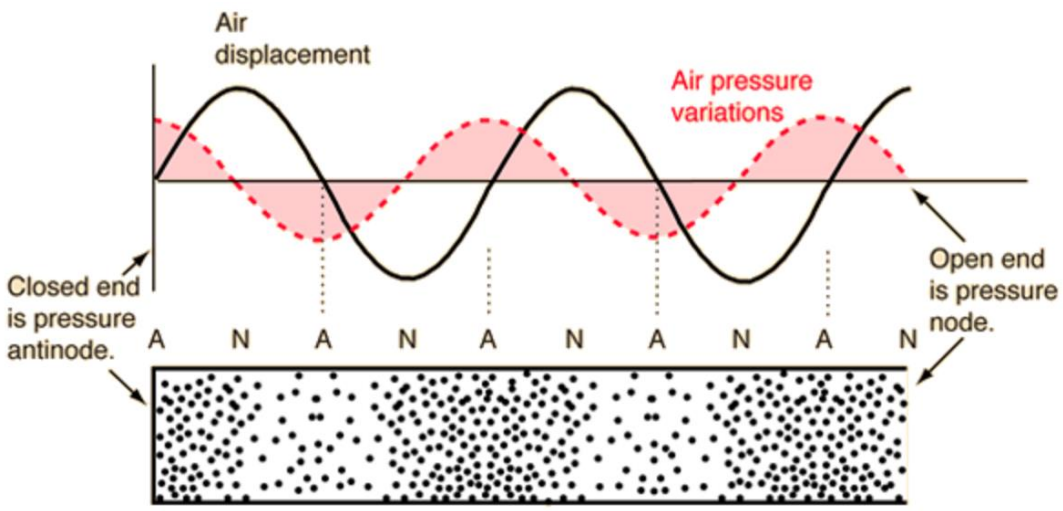


**Figure 30.** The tube (below) is a close-open air column, the black sinusoidal line is air molecules displacement, and the red-dashed one is air pressure. Both of these graphs are standing waves and oscillate. Therefore, the mountains and valleys (positive and negative amplitudes) are changing their positions but nodes remain node. [44]

## 3.4 Wave propagation conditions

The wave speed is related to the wave frequency and wavelength [48].

$$v = f\lambda \tag{13}$$

Equation (13) shows that the velocity of wave ($v$) depends on the frequency ($f$) and wavelength ($\lambda$). In each media at a specific temperature, the speed of propagating wave is almost constant. Therefore, by increasing the vibration frequency, the wavelength will be deepest and vice versa. [48]

Here the function of the standing wave is defined based on air columns. Three types of air column ends are available: open-close, open-open, and close-close. This work deals with open-close and open-open ends because of their functionality in this project. [44]

In an air column, the wavelength and frequency are related to the column's length. For close-open air column, they are based on below equations. [44]

$$\lambda_n = \frac{4L}{(2n-1)} \tag{14}$$

$$f_n = \frac{(2n-1)v}{4L} \tag{15}$$

In both equations, *n* is the number of harmonics or mode shapes (*n*=1, 2, 3 …). By selecting the value of *n*, frequency and the wavelength at that harmonic can be calculated, and *L* is the column length. [44] Figure 31 describes the pressure condition and the molecules situation in an open-open ends column.

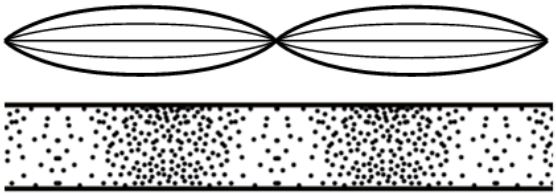

**Figure 31.** (Up) The pressure condition, (Down) the molecules situation at an open-open ends column [44,49].

Both closed and opened end columns have the same equations for wavelength and frequency. [44]

$$\lambda_n = \frac{2L}{n} \tag{16}$$

$$f_n = \frac{nv}{2L} \tag{17}$$

The level of the maximum pressure at the pressure antinodes (displacement nodes) can be calculated from below equation [50].

$$\Delta P_{Max} = \rho v f S_{Max} \tag{18}$$

## 3.5 Effect of boundary condition

The boundary condition determines the standing waves. Therefore, by controlling the boundary conditions, the harmonic or mode shape can be controlled. In Figure 32, the harmonic is defined by an excitation frequency (equal in both cases), the string length, the tension or weight of the ball (which is different for each case, because of different buoyancy forces), and the string density. Tension is a kind of boundary condition affected by different media viscosity and density. [51]

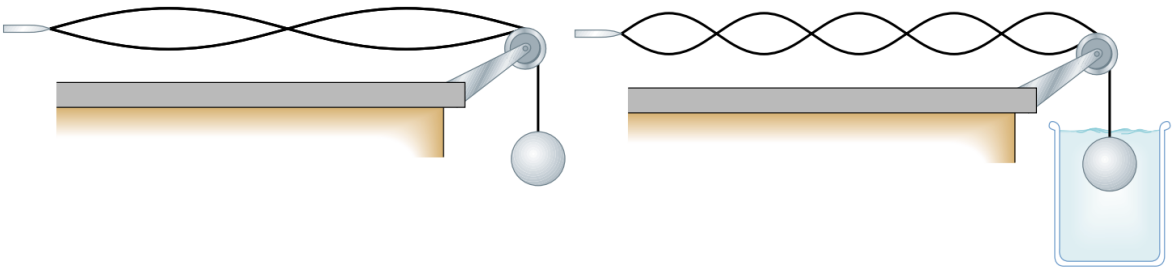

**Figure 32.** (left) the weight suspended in the air activates the second harmonic, (right) the weight in water activates the fifth harmonic [51].

## 3.6 Ultrasonic dehydration

The moisture content of any material can be extracted as a liquid or gaseous fluid. Internal and external resistances resist this process. Therefore, any action that has a reduction effect on these resistances will improve the moisture migration and extraction. [52]

High power ultrasound has a resistance reduction effect, so it assists the dehydration process. Ultrasound, as a sort of mechanical vibrations and waves, travels inside a material and these traveling vibrations produce different micro-stirring and mass transfer effects like atomization, sponge effect, and cavitation. [52]

In solids, a material's characteristics and its temperature define the internal resistance. On the other side, external resistance is related to external mass transfer that is a function of boundary layer thickness. High-pressure waves, that form high intensity ultrasound, have positive effect on increasing the kinetics of mass transfer. [52]

High intensity ultrasound increases the bulk transport of liquid and agitates it, these lead to decreasing external resistance. Another ultrasonic effective mechanism is micro agitation or stirring at the solid liquid interface that reduces the diffusion boundary layer thickness. The intensity of implemented ultrasound has a direct influence on evaporation. Arkangel'skii and Statnikov (1973) found the intensity threshold at 140 dB, they described when intensity of ultrasound goes higher than this threshold its effect increases and for lower intensity minimal or no effect was observed. Furthermore, ultrasound influences both internal and external resistances in front of the moisture extraction. [52]

An important befit of ultrasound dehydration, that makes it a promising dehydration method, is that the effect of ultrasound is higher at lower temperature than higher ones [53].

## 3.7 Ultrasonic effective mechanisms in water extraction

In the following, some of the main effects of ultrasound are presented as atomization, cavitation, sponge effect, and micro channel creation. However, as the lack experimental evidence in this field it is not possible yet to determine which of these mechanisms are more involved in water extraction process. [54]

### 3.7.1 Ultrasonic atomization

Atomization is translating water into small droplets like mist or fog in the gas phase. This process can be happen on the solid liquid mixtures when the moisture content leaks out to the surface and it is subjected to adequate amount of surface disturbances in the normal direction that get moisture separate from the solid surface and disintegrate it into tiny droplets. [55]

As a more detail definition, atomization happens when droplets are vibrated at the appropriate frequency and amplitude to make up resonance condition. As a result, capillary waves are produced on the shell of the droplets, which vibrate with bigger and bigger amplitudes. Smaller secondary droplets eject from the surface. If the resonance frequency of the water particles increases, it will result in faster ejections of water particles or atomization. [56]

Figure 33 shows the sequence of atomization process. A drop of water with about 8 mm in diameter is shown vibrating on an oscillating diaphragm with a fixed frequency, but the excitation amplitude is increasing gradually to induce resonance condition in the drop. [56]

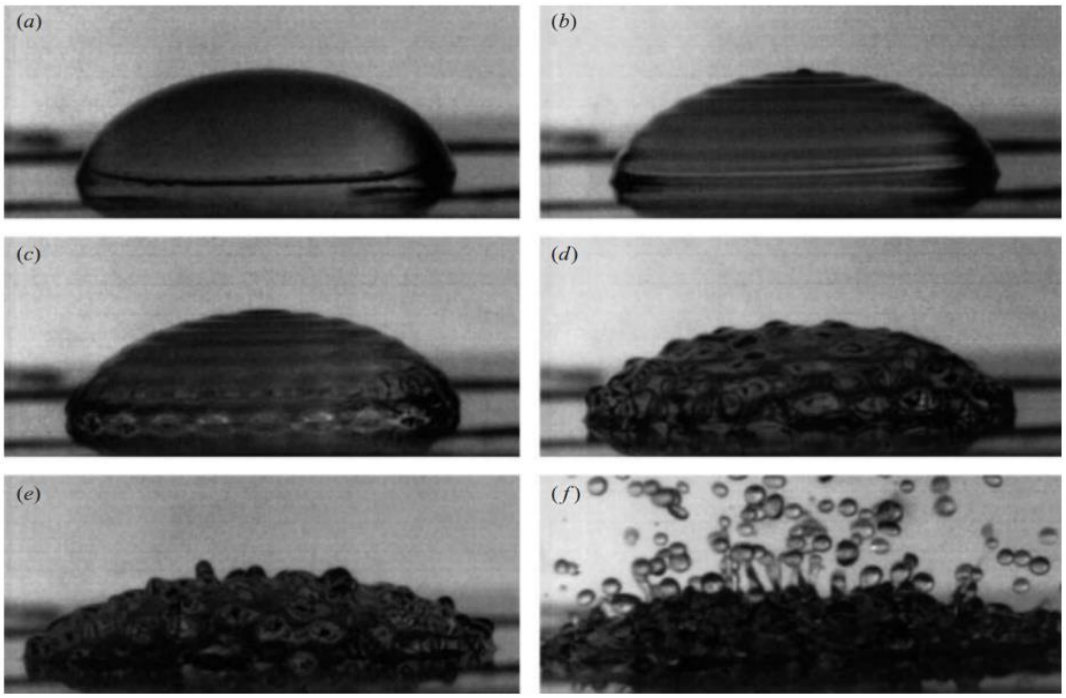


**Figure 33.** (a) The drop at rest, (b) as result of low amplitude, axisymmetric standing waves are created on the surface, (c) stationary and then azimuthal waves on the surface, (d) higher level of time dependent wave motion, (e) growing time dependent craters, (f) fast ejection of small secondary droplets (atomization) [56].

Different methods were used in the past to atomize liquid that worked based on pressurizing liquid or busting its kinetics to split it into smaller droplets. However, there was no control of the size of the droplets in any of them. One problem was that after atomization droplets coalesced or joined together and made bigger drops. A new approach that avoids coalescence and makes the droplets smaller in size is using ultrasound. In addition, ultrasonic atomization uses less energy than the old methods. [55]

The normal frequency for atomizing a liquid layer is between 50 – 3000 kHz. Figure 34 shows an industrial dewatering machine that relies on atomization of moisture content and schematics of atomization process on an ultrasonic nozzle. [55]

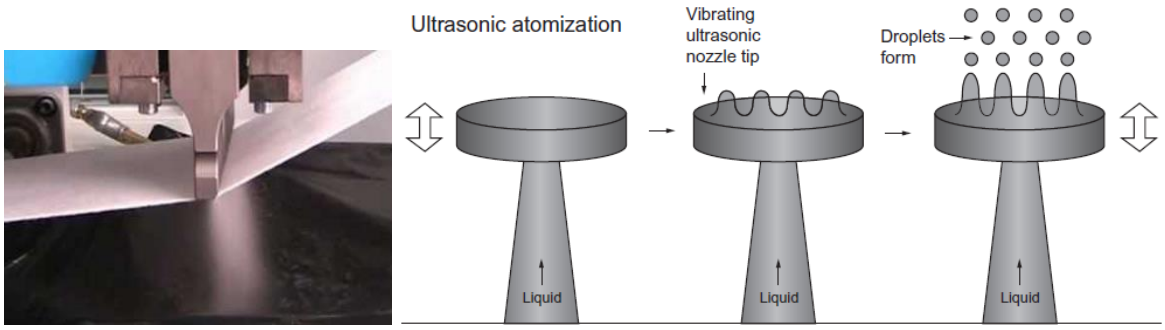


**Figure 34.** (left) Atomization dewatering [57]; (right) atomization phenomenon on an ultrasonic spray nozzle [55].

### 3.7.2 Ultrasonic sponge effect

The mechanical nature of ultrasound is a combination of sequential rapid compressions and rarefactions (changing in pressure), and these oscillatory changes in pressure make a solid material like a sponge that is rapidly squeezed and released (the sponge effect) [52].

The sponge effect can push out or suck in the liquid from the material texture. In other words, the sponge effect makes the micro channels capable for fluid movement and consequentially decreases the internal resistance. [52] Figure 35 shows the schematics of the sponge effect.

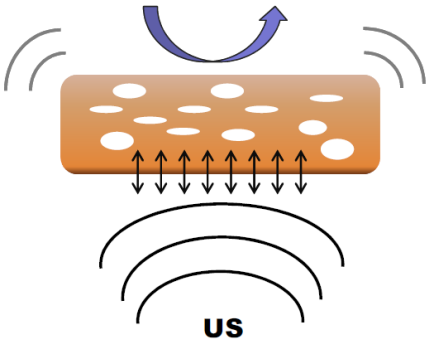


**Figure 35.** Schematics of the sponge effect [58].

If the resultant forces from these mechanical compressions and rarefactions became higher than the surface tension, which holds moisture inside the capillaries and micro-channels, they may assist the water removal process. Furthermore, the pressure fluctuation improves the evaporation rate also. [54]

### 3.7.3 Production of micro channels

High power ultrasound can deform the structure of porous materials and distributes micro-channels inside them. This phenomenon assists the convective mass transfer with reducing

the internal resistance and decreases the boundary layer thickness. In addition, high power ultrasound by changing the material texture increases the cross section area. [54]

The created microscopic channels can work as ways for water particles to escape from the internal parts of the material toward the surface. The amount and dimension of channels, as length and width, are effective options on the level of mass transfer. Furthermore, microscopic channels assist the moisture's diffusion. Based on Fabiano and Sueli experiments on fruit drying, short micro channels did not improve mass transfer but long ones improved it. Figure 36 shows the micro channels creation and region in strawberry and kiwifruit. [59]

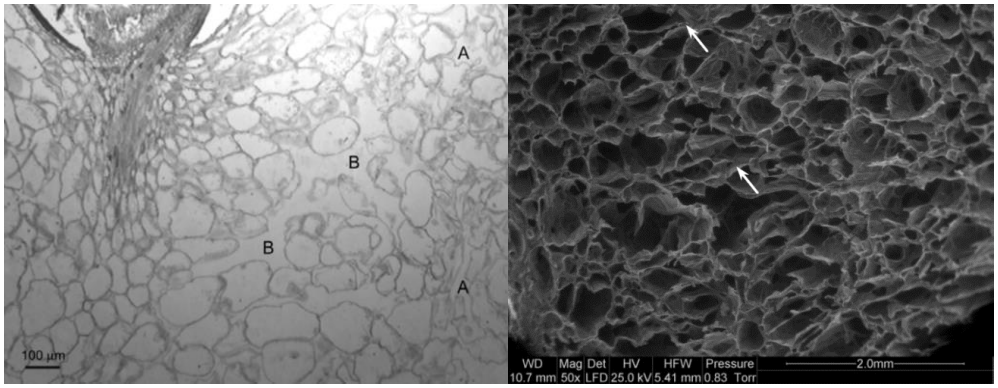


**Figure 36.** (left) Micro channels creation (A) and micro channels regions in strawberry (B) [59]; (right) micro channel creation in kiwifruit [60].

### 3.7.4 Ultrasonic cavitation

Two possible ways to translate any liquid into its metastable condition are either by heating it up higher than its boiling point or stretching it below its saturated vapor pressure that results in returning to equilibrium via vapor bubble nucleation or cavitation phenomenon. Cavitation phenomenon is not known completely but four theories are available that try to explain it: Hot spot, Electrical, Plasma, and Supercritical theories. Between them, hot spot theory is the more acceptable. Ultrasound can induce cavitation phenomenon. [61]

Cavitation consists of production, growth, and collapse of microscopic bubbles in a liquid that generate high local heat energy as well as shock waves and micro jets, which produce turbulence and shear forces that promote mass transfer. The resultant temperature and pressure are up to several thousands of Kelvin and bars. Based on hot spot theory,

temperature and pressure reach about 5000 Kelvin and 500 atmospheres, respectively, during the final collapse. [61]

Figure 37 shows bubble growth until reaches the critical or resonance size. As depicted, bubble osculates in phase with the applied vibration. At each rarefaction, it is expanded and at each compression, it is contracted. [61]

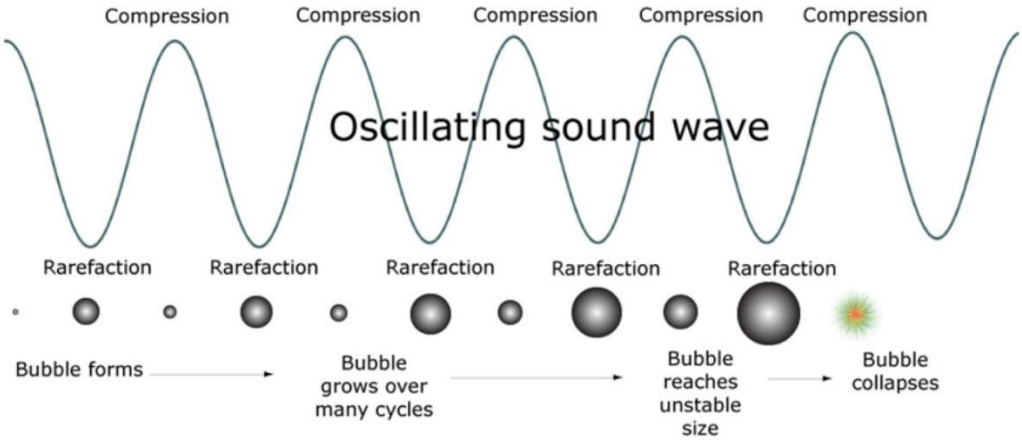


**Figure 37.** Sequence of bubble formation and oscillatory contraction and expansion by the applied frequency [61].

The resonance size is defined by the applied ultrasonic frequency, and then if bubble becomes unstable it will burst. Here is a simple formula that roughly shows the relation between resonance size of the bubble and applied frequency. This formula is approximate, just to have a feeling of bubble size and frequency. [61]

$$f.Rb \approx 3 \tag{19}$$

In Equation (19), *Rb* is the bubble radius in meter [61].

The bubbles generated at 20 kHz frequency are rather large and have powerful bursts and shockwaves. On the contrary, at frequencies of 100-1000 kHz, the resonance size is smaller, but they produce more heat. And, over the 1000 kHz cavitation is too weak (this frequency is used for cleaning fragile electronics equipment). Higher frequencies are used in imaging for medical and industrial reasons. [61]

Near the solid liquid interface, cavitation is symmetric and hits the solid part via its strong and destructive micro-jet, which results in the destruction of pumps and marine propellers. On the contrary, this micro jet is used as a useful agent for cleaning purposes. [54]

However, based on system characteristics, sometimes these bubbles do not collapse and just carry the vibration in the same frequency and the translated vibration helps to agitate mechanically the liquid solution. Furthermore, cavitation may help to extract the strong attached moisture to the solid particles. [52]

The collapsing time is short (just a few μs) and it occurs more on phase boundary. Some factors are effective in lowering the cavitation threshold as low viscosity of liquid content, fractures and discontinuity in solid part, and low surface roughness of container (as cavitation takes place more on boundary layer). [62]

One of the benefits of drying sludge using high temperature is that harmful bacteria and microorganisms available inside the sludge will be eradicated. In dewatering using high power, ultrasound cavitation performs the same task. Cavitation's micro explosions destroy the bacteria and membrane of microorganisms, but the amount of bacteria eradication with high power ultrasound is not evaluated on sludge. To perform effectively bacteria purification, ultrasonic frequency should be selected in the range of 16 - 50 kHz, based on some experiment the frequency of 23 kHz is the most effective one for this purpose. [62]

At one investigation, it was demonstrated that the initial evaporation and vapor bubble growth rate at the presence of cavitation increases 35 times more than the initial evaporation without cavitation [63]. Therefore, it can be concluded that ultrasound will improve drying speed also.

## 3.8 Ultrasonic equipment

In ultrasonic assisted dewatering two main parts of the process equipment are ultrasonic transducers and vibration plate of high power ultrasonic transducer.

### 3.8.1 Ultrasonic transducers

The main part of an ultrasonic system is the generator. The generator produces high-frequency vibration from an energy source such as electronic, magnetic, or kinetic. It consists of an electronic system and a transducer. [52]

Transducers have three main types: electromechanical transducers (piezoelectric and magnetostrictive), liquid driven, and gas driven transducers [64].

*Piezoelectric transducer:* Piezoelectric material works based on piezoelectric effect in a solid material, the effect is the connection between mechanical stress and electrical voltage. The amount of change in shape is up to 4% in volume. Figure 38 shows the schematic motion of a piezoelectric material or piezoelectric effect. [65]

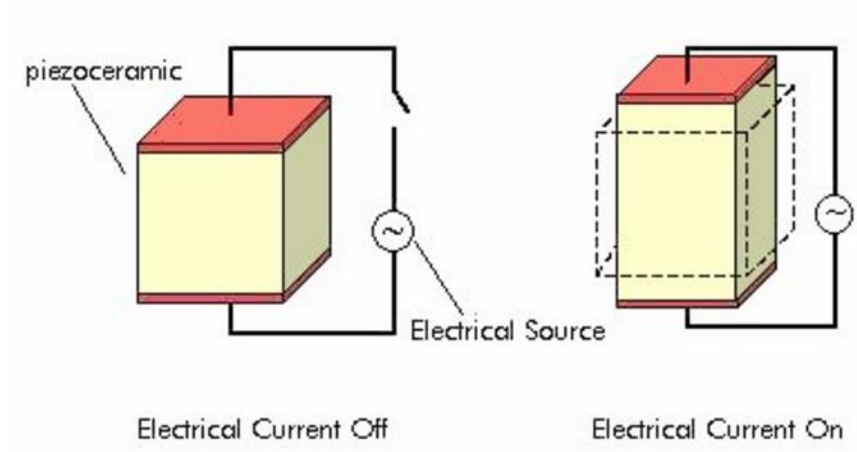


**Figure 38.** Schematic of piezoelectric effect [65].

A piezoelectric material is like an electrical motor, it is possible to give voltage and get motion or like a generator give motion and take electricity. Therefore, they are used for both generating and detecting ultrasonic vibration. [65]

Piezoelectric materials are non-conductive. Two main types of these materials are crystals and ceramics. Quartz clocks and car's airbags work using these materials. In car's airbag, a piezoelectric detector senses the shock of accident and sends an electrical signal to activate airbag. These types of transducers are more efficient than the magnetostrictive ones. [65]

Quartz, a type of crystal materials, is a mechanically fragile material and has low machine ability (hard for machining). Therefore, ceramics are more used recently. Ceramics are in powder shape so are manufactured by grounding and sintering under high pressure and temperature, above 1000°C. [64]

Flange shape ceramics are the most common form. The arrangement method is one disc of ceramic and a flange shape metal to serve both as a protection for ceramics and prevent them from overheating. [64] Figure 39 shows a schematic of arrangement and a sample of sandwich assembly.

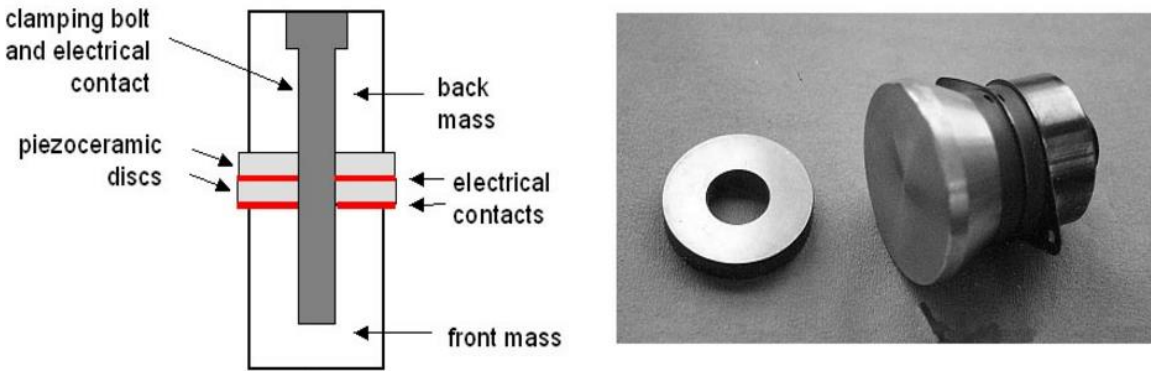


**Figure 39.** Disc shape ceramics and flange shape metals arrangement [64].

The thickness of an assembly should be an add multiple of half a wavelengths, like 5λ/2, 7λ/2, and so on. Figure 40 shows the graphical meaning of half a wavelength. These transducers have high efficiency (over 95%) and the level of piezoelectric frequency reaches up to 150 MHz (Megahertz). [66]

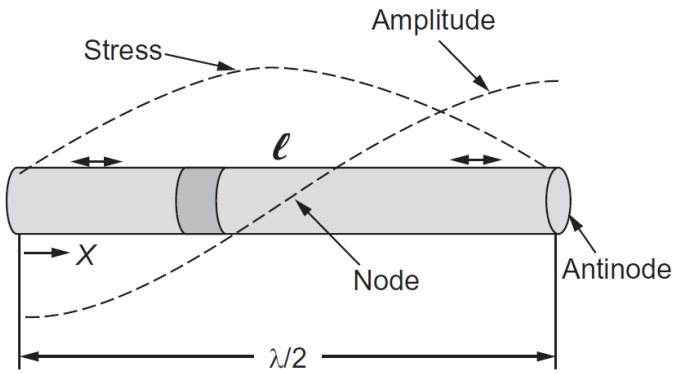


**Figure 40.** Graphical meaning of half a wavelength [66].

*Magnetostrictive transducer:* this type of transducer is the first one that was used on industry for high power ultrasound generation. The basic of function is using from materials like Nickel that reduces in size when located in a magnetic field. When magnetic field sequentially applied, its size will be changed as the same frequency (vibrate as the same frequency). In other words, it works like a solenoid. Magnetostrictive material forms the core and copper wire winding around it. To tackle the magnet losses, a couple of these cores

and wires are connected in a loop shape. Figure 41 shows a magnetostrictive transducer and its schematics. [64]

These types of transducers are durable but there frequency is limited up to 100 kHz and the other disadvantage is their low efficiency about 60%. The other 40% is translated into heat energy so they always need king of cooling system. However still for heavy industrial applications magnetostrictive are used. [64]

To improve the efficiency old Nickel core can be replaced with Cobalt-Iron, Aluminum-Iron, or TERFINOL-D [64].

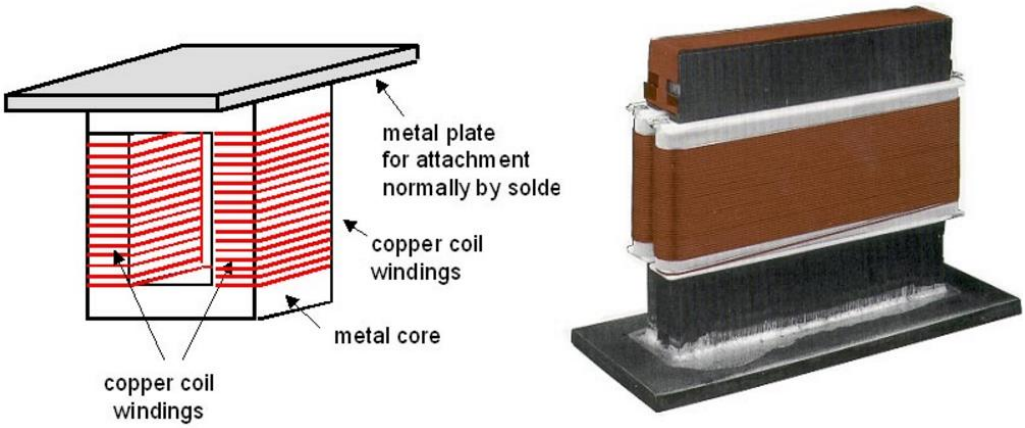


**Figure 41.** A magnetostrictive transducer schematic (left), a sample of it (right) [64].

*Liquid driven transducer:* In this type of transducer, the oscillation is created via kinetic energy of a fluid. This transducer is like a liquid whistle and works via generating cavitation. [64]

In these systems, heterogeneous mixture is forced at high velocity through an adjustable channel that makes the fluid in a jet form and hits the vibrating steel blade. Cavitation happens firstly as the sudden expansion of liquid after the orifice and then because of the high frequency vibration of the blade. [64] Figure 42 shows a graph of liquid driven transducer.

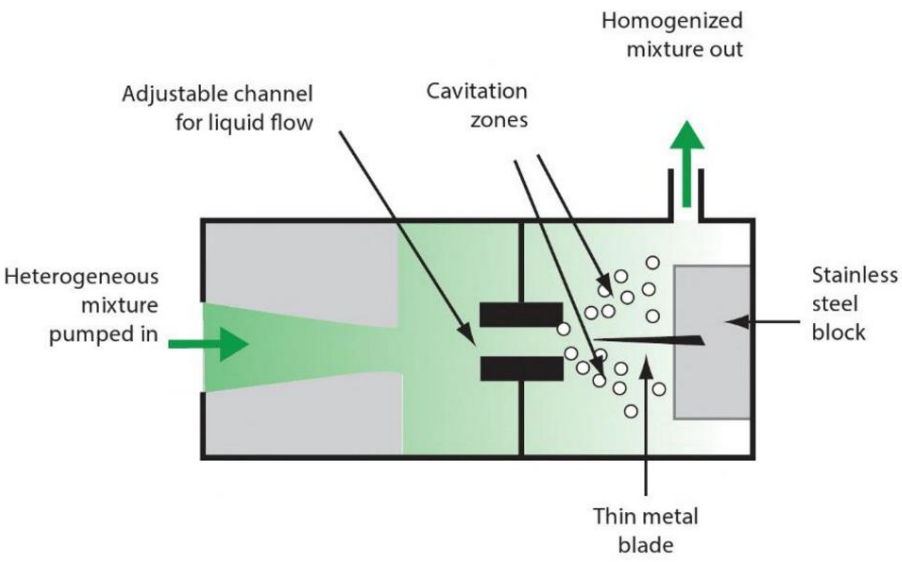


**Figure 42.** Graph of liquid driven transducer [64].

*Gas driven transducer:* This type of transducer has a limited application. It is a simple whistle that produces high frequency. [64]

### 3.8.2 Vibrating plate of high power ultrasonic transducers

The main requirement for transducer vibration plate is robustness. The most common type of high power transducers are based on piezoelectric sandwich transducer designed by Langevin (1920) that has typical limitation in power and size. [67]

In air borne transducers, the impedance mismatch problem can be addressed via increasing the radiating surface area of the transducer because of proportionality between radiation impedance and the radiator surface [67]. Figure 43 shows the basic structure of a plate transducer.

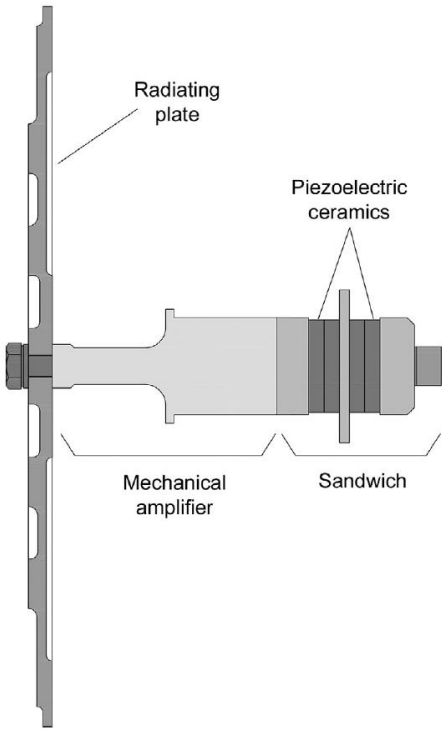


**Figure 43.** Basic structure of a plate transducer [67].

A plate transducer as depicted in Figure 43 consists of a radiator that is driven by a piezo electrically activated vibrator, which is a combination of piezoelectric stack and a solid horn. The solid horn amplifies the vibration. This assembly, piezoelectric stack amplifier, vibrates the radiator in one of its flexural modes. The shape of the radiator could be either circular or rectangular plate with stepped profile. [67]

To get the first length approximation of the vibrator assembly, the design of piezoelectric sandwich and horn is calculated in the form that all the components make up a length that is half of the extensionally propagated wavelength through it [67].

In a vibrator assembly to increase the fatigue strength, have better coupling on the assembled parts of a vibrator, and reduce mechanical losses a pre-stress of 250 kg/cm$^2$ is applied via a central screw in piezoelectric sandwich [67].

The vibration modes of vibrator are determined via modal analysis. The operating or tuned mode frequency is determined along with nearby harmonics and modes. According to Gallego [67] “The resonance is calculated under a short-circuit condition, where a constant

voltage of zero is applied at all electrical contacts of the ceramic stacks, while the anti-resonance is calculated under open circuit conditions." Figure 44 shows the operating mode shape and nodes in a vibrator.

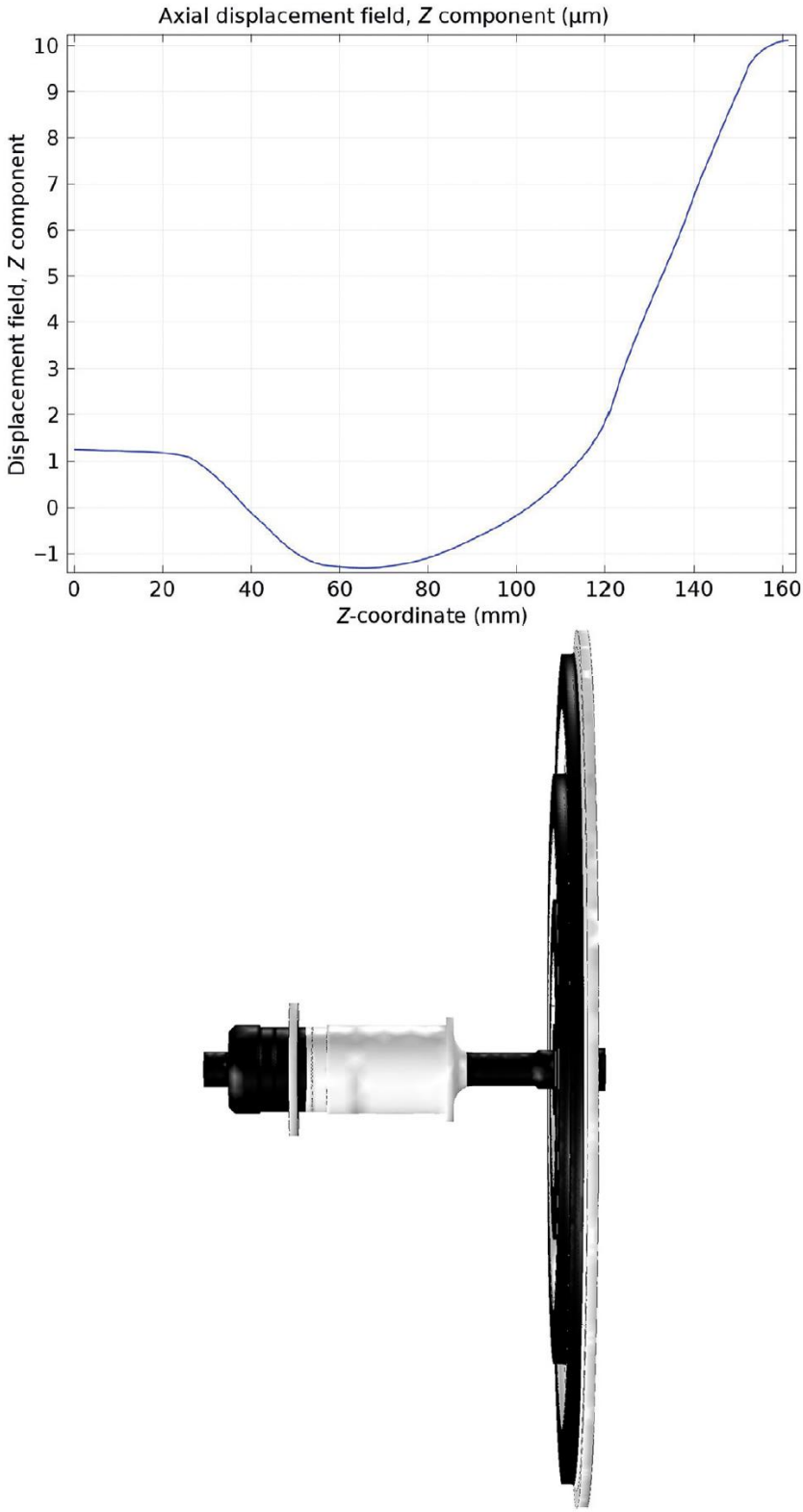


**Figure 44.** Operating mode shape and location of nodes [67].

The main objective of stepped profile design is to arrange in phase the radiation waves across the plate, phase coherent effect. To have phase coherent effect the vibrating surface elements that are in counter-phase on the sides of nodal lines (for rectangular plates) or circles (for circular plates) should be shifted for half a wavelength in the direction of wave propagation, as illustrated in Figure 45. The effect can be shown when the acoustic pattern of stepped plate and flat plate are measured and compared. [67]

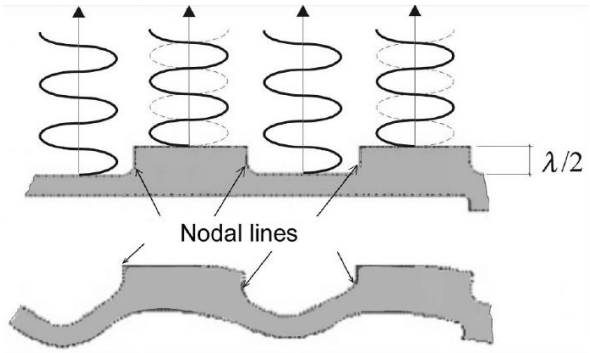


**Figure 45.** Producing phase coherent in propagating wave by stepped surface [67].

In some specific industrial applications, rectangular transducers may have technical and practical advantages over the circular ones, because of their more uniform vibration distribution. Rectangular plates deform in sine and cosine function shape. These deformations are more uniform in the central and outer areas. [67]

Rectangular radiators are the main demands in large-scale industrial applications, because they generate more uniform acoustic field and vibration distribution with smoother stress that consequently improves fatigue resistance and power capacity. Both faces of these plates are stepped to generate directional radiation from both sides. Figure 46 shows two samples of rectangular vibrating plates. [67]

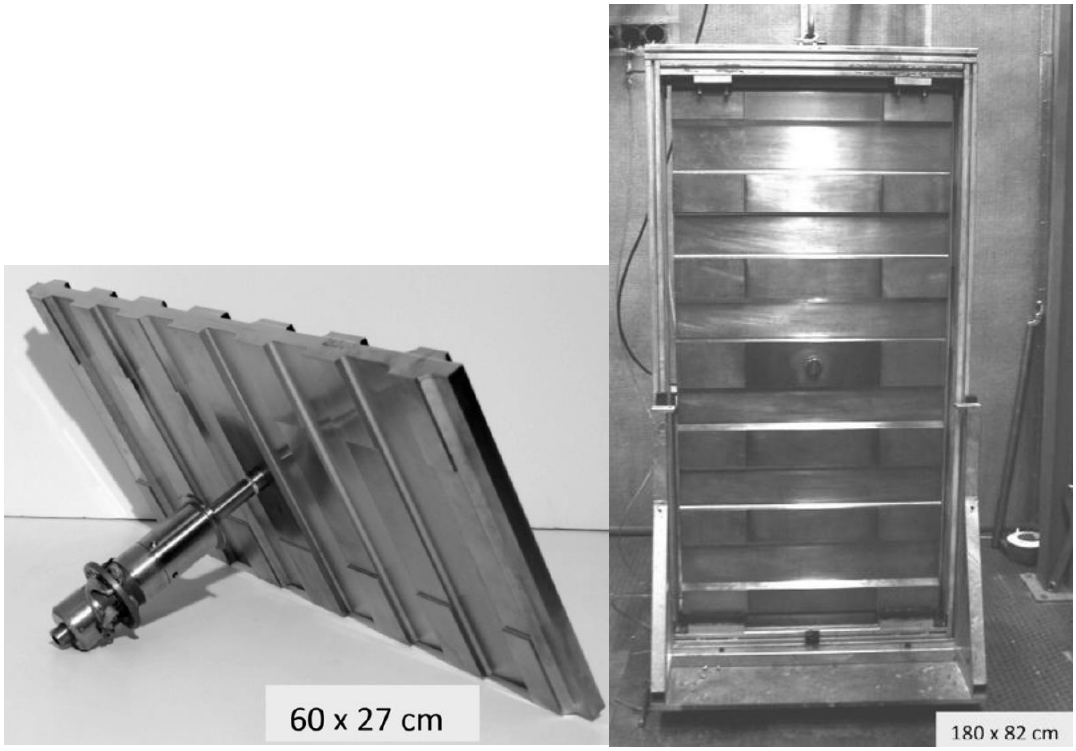


**Figure 46.** Two stepped plate rectangular vibrating plates in different sizes [67].

## 3.9 Ultrasonic-assisted dehydrations

Available mechanical dewatering methods cannot completely extract the moisture of sludge. It seems that by assisting dewatering with high power ultrasound and take advantage from the sponge effect, atomization, cavitation, and microchannel propagation it could be possible to enhance mechanical dewatering.

### 3.9.1 Rotary vacuum dewatering + ultrasound

Figure 47 depicts the implementation of high power ultrasound on a rotary vacuum for dewatering $TiO_2$ with particle size about 1 µm. Here the ultrasonic vibrating plate is almost in direct contact with sludge. It was demonstrated that ultrasound effectively increases the moisture migration. [68]

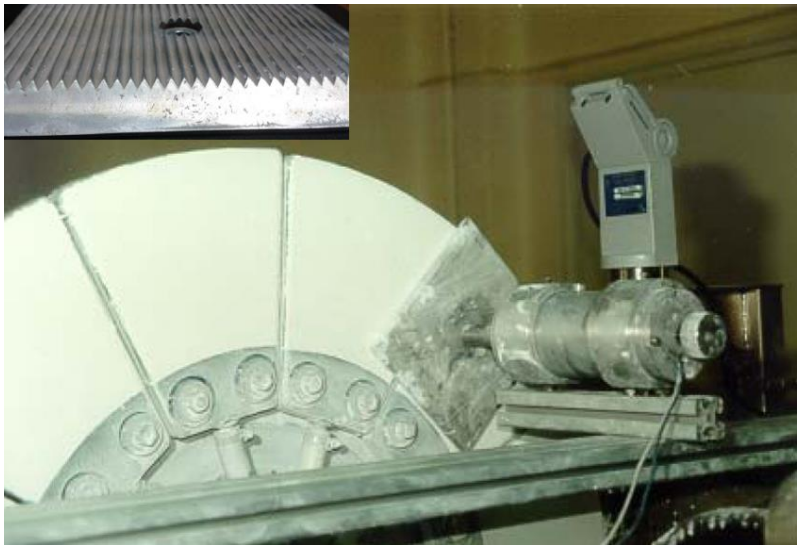

**Figure 47.** Implementation of high power ultrasound on a rotary vacuum dewatering, (up left) the vibration plate profile [69].

The normal steps in rotary vacuum dewatering are: cake formation via filtration, water extraction from cake, and finally cake discharging. In this experiment, the high power ultrasound works on the second step of the process (water extraction). [68]

In this system the vibration plate, placed parallel to the rotating filter surface, is driven close to the filter cake, and it touches the cake during its operation. Because of this physical contact, an acoustic coupling is created that boosts the ultrasonic energy penetration. [70]
In this experiment, different acoustic powers were tried from 0.1 to 1 $W/m^2$ and grate results came out. It was demonstrated that by using a relatively low power ultrasound transducer, 60W of power, at a short period of time, just 2 seconds, cake TS was improved by 6%. When the time effect increased, the results improvement doubled. [70]

### 3.9.2 Drying + ultrasound

In food industry, dehydration using hot air drying and freeze-drying are methods that are more popular. For freeze drying first the product is frozen then the ice is sublimated that maintains quality but it is an expensive work. On the contrary, hot air drying produces deteriorative changes in product and is more economical. [71]

According to Gallego-Juárez [71] "The application of air-borne ultrasonic energy for drying materials has been explored for several decades. Nevertheless, a few air-coupled ultrasonic

dryer were reported in the technical literature and apparently none of them was used in large-scale industrial plants The main difficulty, apart from the generation problems, is the transfer of acoustic energy from air into the product due to the acoustic impedance mismatch. Then the major effect is produced at the liquid/gas interface."

The following experiments compare the forced convection drying of carrot at high temperatures to ultrasonic-assisted forced convection at ambient temperature when the high frequency vibrating plate is in direct contact with the drying material. Stepped plate ultrasonic transducers normally vibrate at the frequency of 20 kHz. A flat plate parallel to the stepped plate works both as the reflector to create standing waves and sample holder. [71]

Ultrasound is more effective at low temperatures and helps only at airflow between 2 to 4 m/s. Moreover, satisfying acoustic match by direct contact between vibrating plate and the drying mater helps the deep penetration of acoustic energy. As described before, ultrasonic mechanisms all or some may help for better migration and extraction of water inside the material. Figure 48 shows the drying kinetic graphs at different temperatures and ultrasonic assisting drying. [71]

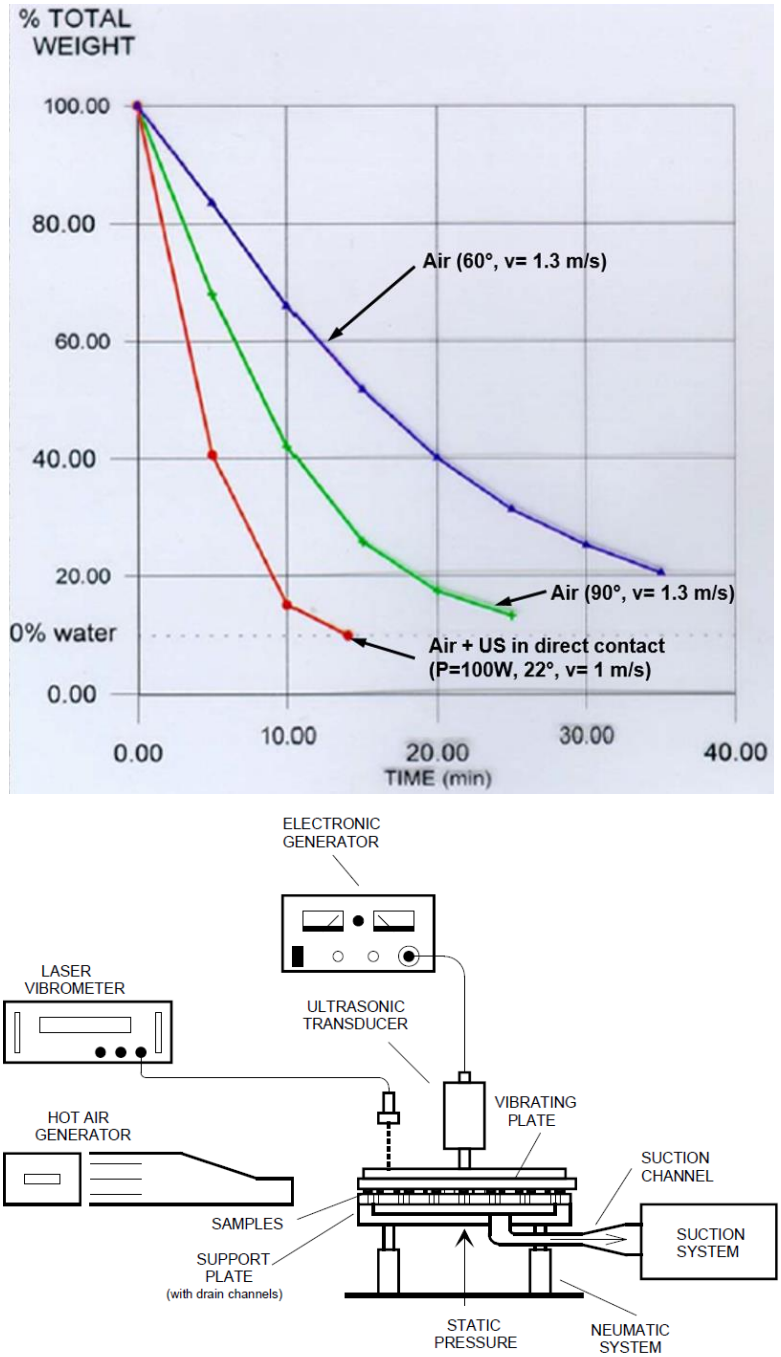


**Figure 48.** (up) Drying kinetic graphs comparison [69]; (down) Schematics of dryer and ultrasound system set up [71].

As demonstrated on the graph, at 22°C with 1 m/s speed of air flow carrot samples were dried faster about 2.3 and 1.7 times in comparison with temperatures of 60°C and 90°C respectively, with air flow of 1.3 m/s. In this system, one effective mechanism is the pressure difference in the dehydration set up, from one side airflow and the other side vacuum (suction system) work to make pressure difference. [71]

# 4 PRACTICAL EXPERIMENTS

At the beginning of this work, it was seemed that the dewatering methods were highly matured and PAKU researches could not find any new ideas regarding dewatering. Therefore, it was adopted to study the experimental drying kinetic under vacuum in comparison to atmospheric drying.

The motivation of the work was an idea regarding drying sludge under vacuum created via a cylinder that is actually the drying chamber also. Figure 49 shows the mechanism of system. However, this idea is perfect for drying materials that are sensitive to high temperatures, because producing vacuum in this method is faster than any other vacuum pump and needs lower energy to produce it.

Nevertheless, as described in "Comparison of vaporization energy requirement with and without vacuum" there is not a big difference in the amount of heat energy consumption, vacuum drying just saves 5% heat energy. Nonetheless, if the energy needed to make vacuum is added, it may be more than atmospheric drying energy consumption.

However, studding the drying kinetics under vacuum and atmospheric pressure helps us a lot to earn some understanding about drying process duration and kinetics.

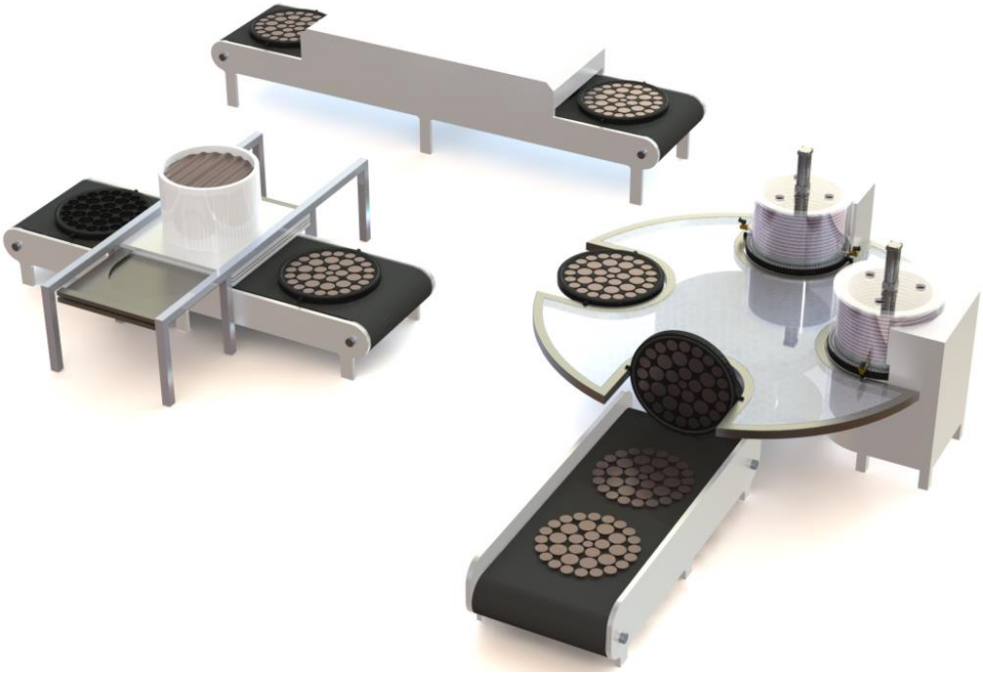

**Figure 49.** Cylindrical vacuum chamber dryer concept.

To implement tests, a vacuum oven (model AccuTemp-19q - Across International) was used to practically evaluate the effect of temperature and vacuum on drying kinetics and final TS. Figure 50 shows the test set up.

**Figure 50.** Test set up of vacuum oven and pump [72].

For drying experiments, cooked rice was selected as a material sample to compare different drying conditions. The reason for this selection was that the mixture of cooked rice, soybean paste, and water is the most normal material to make fake human waste, which makes up the main material inside the municipal sludge. The main ingredients in fake human waste are water and rice. [73]

Making rice procedure as the test spacemen

The spacemen to test drying process should be homogenous in all the experiments. Therefore, it is highly critical to follow the same process for its preparation.

The ratio of water to rice for cooking is 5 to 1 so for each pack of specimen 50 gm of rice and 5 time more water (250 gm) at moderate temperature are used. The knob top valve of the stove that is in use for cooking is graduated from 0 to 6.

The below steps have been passed to make rice for all the experiments, the timing in parentheses are based on stopwatch for time measurement:

1. On grade 6 of knob valve for 7 min to start boiling with open lid (0-7 min)
2. On grade 1 of knob valve for 7 min to stop boiling with open lid (7-14 min)
3. On grade 1 of knob valve for 7 min with closed lid (14-21 min)
4. On grade 1 of knob valve for 1 min with open lid (21-22 min)
5. On grade 1 of knob valve for 12 min with closed lid (22-34 min)
6. On grade 1 of knob valve for 5 min with open lid (34-39 min)
7. At 39 min, translate pot from oven to the counter.
8. Wait for 1 min. (39-40 min)
9. Mix the rice for 1 min, to make it more homogenous. (40-41 min)
10. After 3 min, translate the rice into a zipper storage bag, to save the moisture content. (at 44 min)

The reason of opening the pot lid in some steps is to tackle the over boiling problem. All the rice preparations are done on the same stove and the same burning pot. In addition, for weighting measurements, always the same scale was used. The resultant cooked rice has about 205 to 210 gm weight. Figure 51 shows a cooked rice pancake sample ready for drying test.

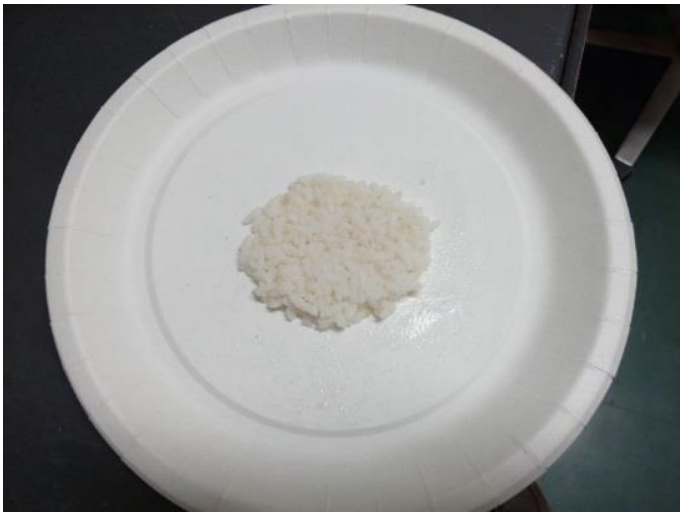

**Figure 51.** A cooked rice sample.

The actual water content of dry rice that was used at the experiments is unclear, and probably subject to change with room humidity. However, as an estimate, dry rice has roughly about 12% moisture (88% TS). Therefore, the result of the rice preparation has approximately around 22% TS. The sludge from the normal dewatering machines has something between 20 to 45% TS (45% using Fournier rotary press based on their data). [18,74]

## 4.1 Drying tests

A set of experiments were decided and conducted at LUT machine design laboratory, in two scenarios of atmospheric pressure and vacuum condition, at temperatures of 40°C, 60°C, 80°C, 100°C, and 120°C.

To carry the material inside the oven, the pancakes are prepared on paper plates using a PTFE die to have the same thickness of rice in all the tests. The weight of each paper plate is 9 gm. In both vacuum and atmospheric drying tests, counting the time is started as soon as the rice pancake is translated from the scale to the oven and in predefined interval times the sample is taken out and weighted, then it is returned into the oven. The process progresses until the weight of rice remains constant. The room temperature was under control about 21°C during the whole experiments.

## 4.2 Atmospheric drying tests

Figure 52 shows the graph of atmospheric drying kinetic results for 5 different temperatures. The times to dry rice pancakes at specified temperatures are listed in Table 8.

*Table 8. Drying temperatures and times for atmospheric test.*

| Results of atmospheric drying tests | | | | | |
|---|---|---|---|---|---|
| Temperature (°C) | 120 | 100 | 80 | 60 | 40 |
| Drying time (min) | 240 | 330 | 420 | 720 | 1305 |

Figure 52 is the drying kinetic graphs for 5 different temperatures in atmospheric drying tests.

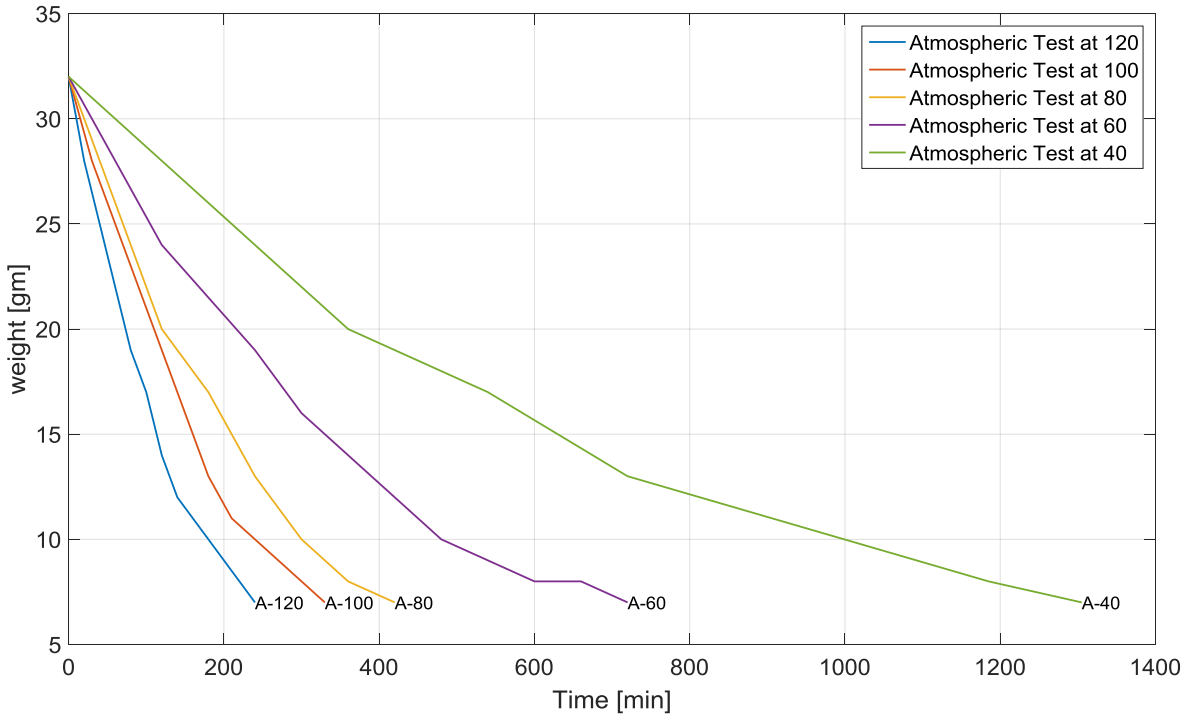


**Figure 52.** Graph of atmospheric drying kinetics – On the graph, (A) labels the atmospheric test, and the number after A is the specific test temperature.

As illustrated, the fastest test takes about 4 hours at 120°C and the slowest one about 21 hours and 45 min at 40°C.

## 4.3 Vacuum drying tests

The times that take for rice pancakes to be dried at specified temperatures in vacuum drying tests are listed in Table 9.

*Table 9. Drying temperatures and times for vacuum test.*

| Results of vacuum drying tests | | | | | |
|---|---|---|---|---|---|
| Temperature (°C) | 120 | 100 | 80 | 60 | 40 |
| Drying time (min) | 150 | 180 | 195 | 240 | 360 |

Figure 53 shows the vacuum drying kinetic results for the 5 different temperatures.

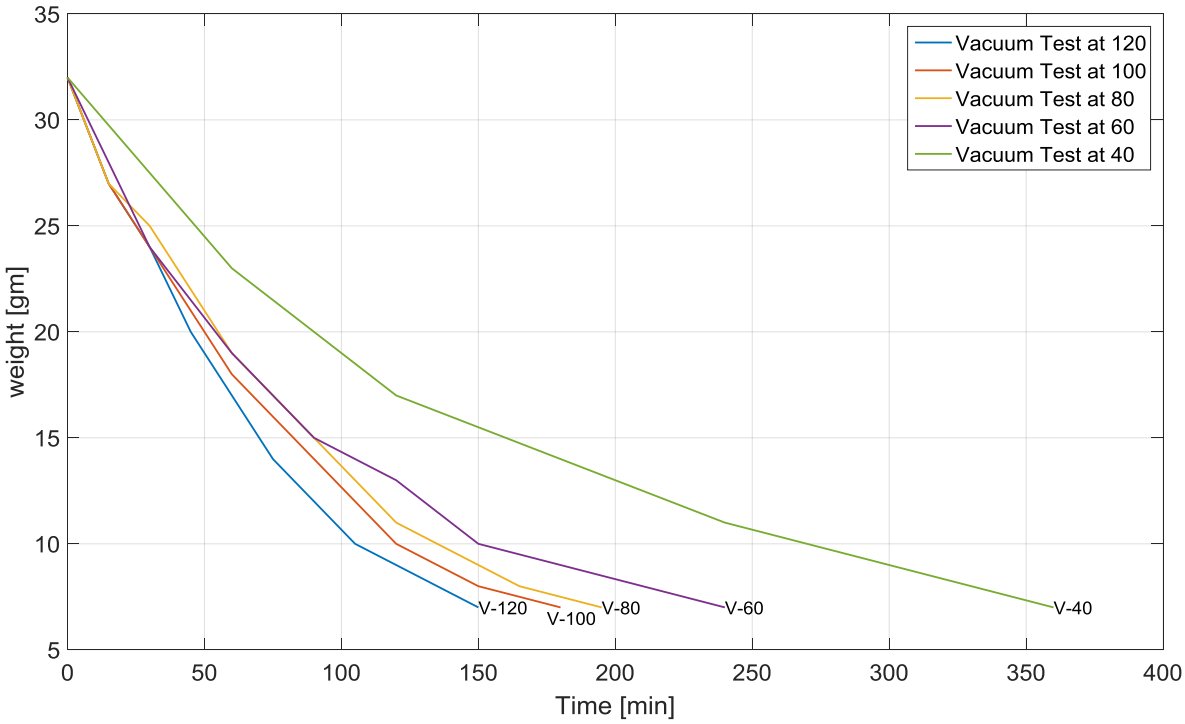


**Figure 53.** Graph of vacuum drying kinetics – On the graph, (V) labels the vacuum test, and the number after V is the specific test temperature.

As illustrated, the fastest test was done in about 150 min at 120°C and the slowest one took about 360 min at 40°C.

## 4.4 Dryness and timing

At these experiments 32 grams of cooked rice for each experiment was used as the drying sample and the drying processes were carried on to reach 7 gm of the weight of rice, it is worth to mention that when the tests continued further, the rice weights never became in weight less than 7 gm.

The results show about 25 gm or 78% of the cooked rice is evaporated as moisture and the rest, 7 gm or 22%, remains (this residual rice still has some water). For comparison, the weight of dried rice in sample preparation was always 50 gm (it has about 12% moisture, so roughly 44 gm TS), and it reached 205-210 gm with 21% of TS and 79% moisture. Therefore, the results were always about the same level of dryness as the primary dried rice just with 1% more moisture, in other words almost all the water added in cooking was extracted at the drying sections.

To have a better image of time difference in vacuum and atmospheric drying, Figure 54 is prepared which shows the timing difference comparison between atmospheric and vacuum tests.

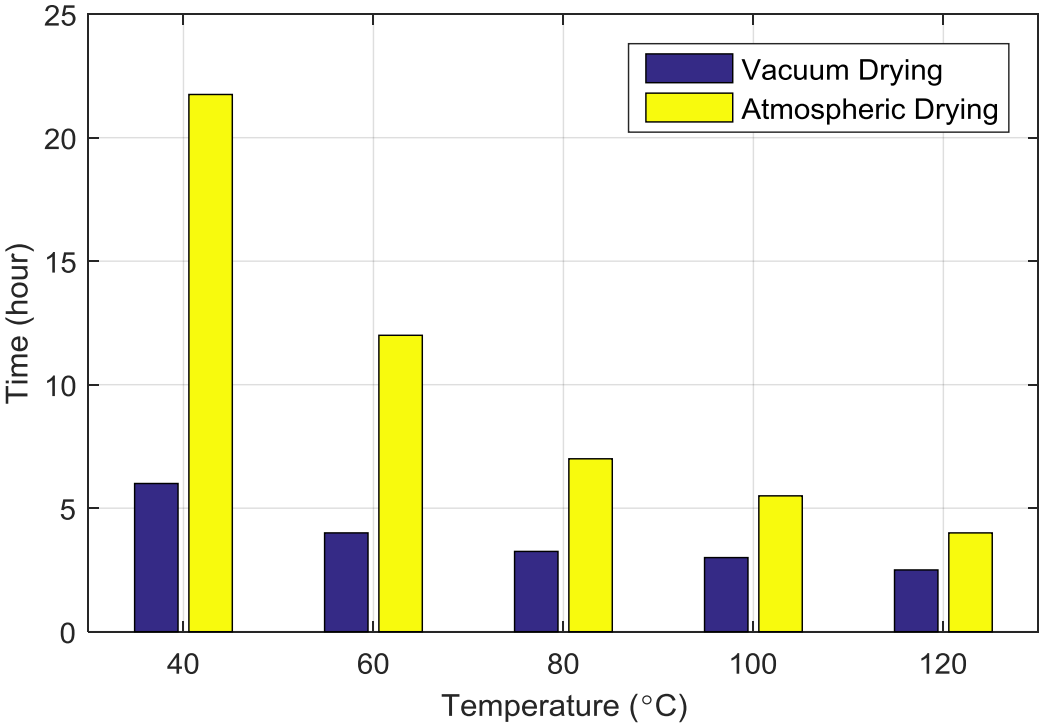


**Figure 54.** Time difference between atmospheric and vacuum tests.

As illustrated in Figure 54 by decreasing temperature the difference between drying times of vacuum and atmospheric increases more.

Figure 55 is the picture of the results of the drying tests.


**Figure 55.** The results of drying tests – (Up row) are the atmospheric dried samples, (Down row) are the vacuum dried ones. The temperatures are written on the plates from the left to right: 40°C, 60°C, 80°C, 100°C, and 120°C. The sample at 40°C in vacuum drying is different from the rest and has a bigger volume but the same weight, because of the low temperature this sample almost freeze-dried.

## 4.5 Ultrasonic dehydration experiment

In the experiments that were done in Spain at Pusonics Co., the same drying sample (cooked rice) was used as the test spacemen in three scenarios. In the first one it was tried to dewater the cooked rice just using airborne ultrasound, in the second one the airborne ultrasound was assisted by warm air flow (forced convection), and in the third experiment to figure out the effect of forced convection on the dehydration process one experiment was done just by using forced convection. In all the experiments the room temperature was under control (20.5°C). At the last experiment (forced convection without ultrasound) may be because of the absent of ultrasonic vibration in the air about the drying sample area temperature increased by 1°C. The worm airflow was implemented via a fan heater. Figure 56 shows the related test setup.


**Figure 56.** (left) Temperature measurement method using three thermometers, (right) drying set up at Pusonics.

The first experiment was pure ultrasound dewatering as no other option was cooperating in drying process.

Figure 57 shows the results of ultrasound dehydration in comparison with the fastest vacuum and atmospheric drying tests.

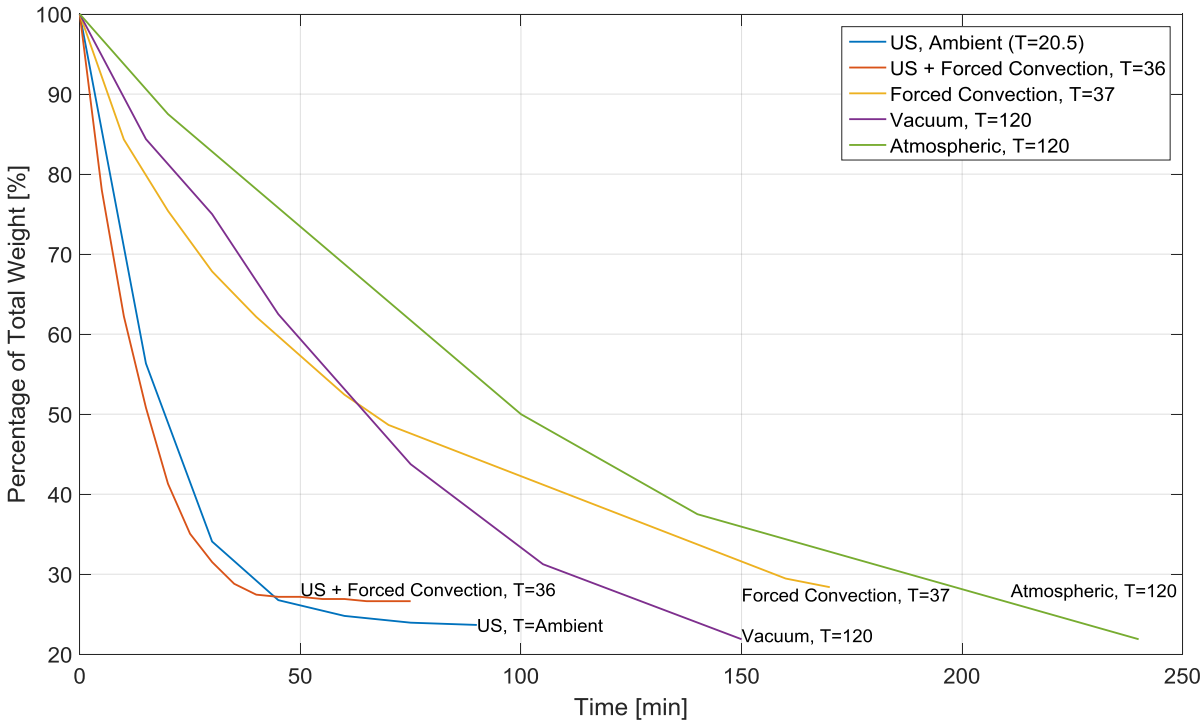


**Figure 57.** The results of ultrasound dehydration and the fastest vacuum and atmospheric drying tests at 120°C – In the picture, US means ultrasound. At the legend, the measured temperatures at any test are illustrated (the ultrasound at ambient took 90 min).

As can be seen on the graph the fastest drying methods are those that use ultrasound, US + forced convection and ultrasound at ambient temperature. The ultrasound + forced convection has better drying kinetics than ultrasound alone but alone ultrasound makes the material drier, the reason could be creation of a dried layer on the surface of rice that isolates the lower layers.

In conclusion, the drying kinetics improved tremendously when ultrasound is used at ambient or low temperature in comparison with other drying methods. Accordingly, it could be judged from the presented data about the dewatering systems and the test results that the only mechanical dewatering method that effectively with the high value of TS extracts the water content is ultrasound.

# 5 DISCUSSION ON ULTRASONIC DEHYDRATION WEAKNESSES

According to the pressure and displacement nodes and antinodes, discussed in the “standing waves” section, some weaknesses are available in the affectivity of the sponge effect, cavitation, atomization, and probably creation of micro-channels.

## 5.1 The sponge effect and cavitation weaknesses

The harmonic motion of the molecules in an air column under sound effect is similar to other materials as liquids, slurries, or even solids. Therefore, it could be possible to discuss based on the standing wave physical principles about the sludge as slurry or unconnected solid particles. Therefore, the method that the particles under the ultrasonic waves are compressed and rarefied follows the standing wave physics.

In ultrasonic dewatering, the pressure variation is the activator of the sponge effect as well as cavitation. As defined in advance, the sponge effect is the sequential pressure variation in a material's field and cavitation is stretching water below its saturated vapor pressure. Based on the air molecules motion and pressure graphs some particles experience the highest pressure variations (pressure antinodes) and some others are in the region of highest physical vibration and experience no pressure differences or are in low pressure effect region (about the pressure nodes). Therefore, pressure antinodes are the main regions that make the sponge effect and cavitation.

To brush up this connotation, Figure 58 shows the pressure wave, displacement wave, and molecular position schematics in an open-close air column. Here vibrating wall side is considered as an open end, highest displacement and no pressure deference.

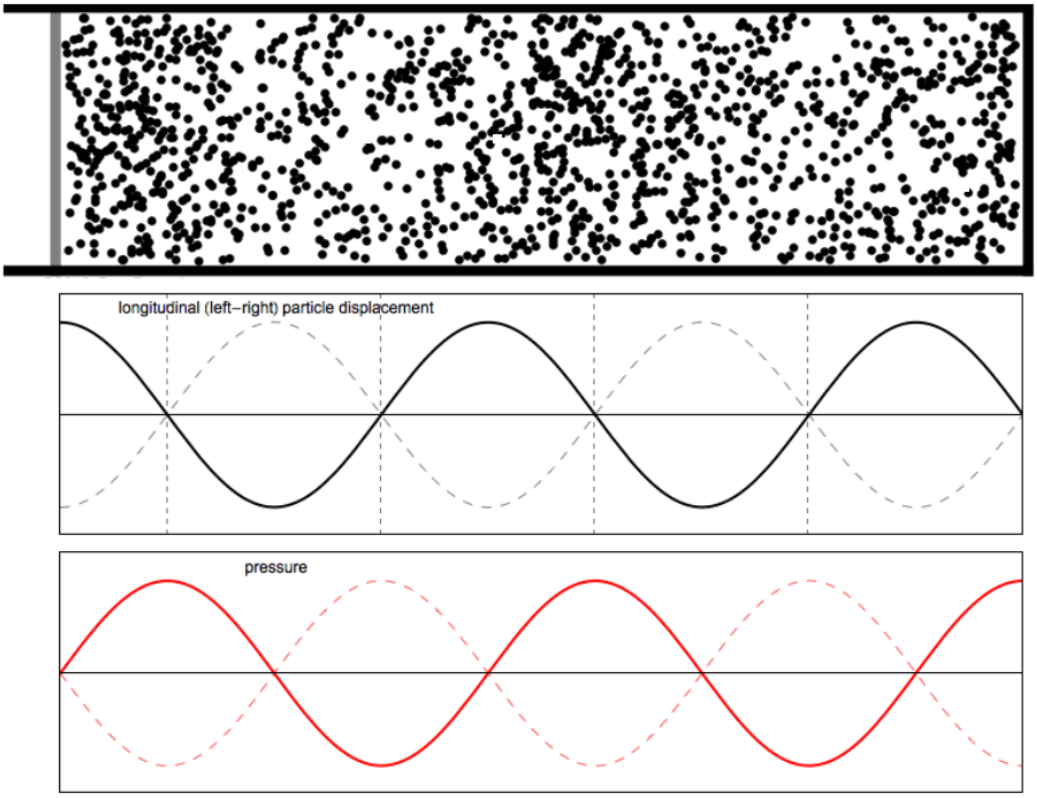


**Figure 58.** From up to down: air column, particle displacement graph, and pressure graph – In the picture of air column, the left gray wall is oscillating back and forth and should be considered as the open end [modified, 75].

Accordingly, as illustrated in Figure 58 and previous discussions, in any field of material under ultrasonic vibration, some layers are under the highest pressure variation and some others do not experience any pressure fluctuation. To be more accurate, about the half of the material is under highest or high-pressure variation, and the rest is under low or no pressure variation, if the thickness of material is a factor of wavelength. Figure 59 shows the high and low-pressure regions in a pressure graph. Therefore, it could be beneficial to activate the pressure nodes also, because the sponge effect and cavitation are not induced in the nodes of pressure graph.

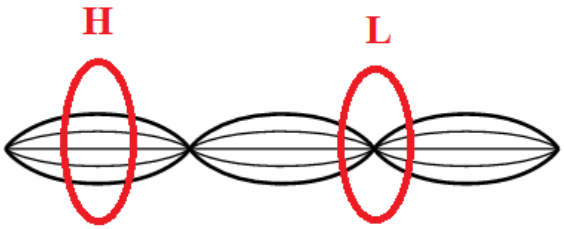


**Figure 59.** High and low pressure regions, H means high pressure and L low pressure [modified, 49].

In conclusion, by activating the pressure nodes, the influence of the sponge effect and cavitation could be increased (the sponge effect and cavitation happen at best, in the extremums of the mountains and valleys of pressure graph).

## 5.2 Atomization weakness

Atomization is inducing liquid to vibrate with enough intensity to be scattered into small droplets, it relies on increasing kinetic energy of water particles. Therefore, it seems the effective regions of the pressure graph are those with little or no sponge effect or cavitation or those where the pressure nodes have the greatest physical motion.

To conclude from the discussed weaknesses, in the presence of the sponge effect and cavitation, the level of atomization is low or nonexistent. And, in the presence of atomization, there is negligible sponge effect or cavitation. Moreover, if atomization occurred in the same regions of the two other effects, the whole material would not be under the effective ultrasonic treatment.

The following data is presented to better understand the practical aspects of wavelength size. In the course of this project, no data about the speed of sound in dewatered sludge was found in the literature. Therefore, the pressure wave speed of sound in wet sand and sewage sludge (before dewatering) has been used. In wet sand, the speed of sound is between 1500 and 2000 m/s [76]. In sewage sludge, it is about 1500 m/s [77].

According to the speed of sound in wet sand and sewage sludge, the wavelength of ultrasound at 20 kHz from standing wave relations is about 7.5-10 cm. In sonographic imaging, high frequencies are used to have shorter wavelength and see more details of the

living tissues [78]. In majority of scientific papers regarding ultrasonic dehydration, the moisture extraction is discussed on microscopic and molecular size. Therefore, it is worth activating the pressure and displacement nodes, because the particles do not change their positions with each other or mixed under the ultrasonic effect and by this work the three main ultrasonic mechanisms work on the entire material. Furthermore, it may generate more channels for moisture migration.

## 5.3 Proposed mechanisms to improve ultrasonic process

These methods are proposed to study dewatering mechanisms under expected conditions to discover the level of their functionality and affectivity to address the uneven ultrasonic mechanisms distribution for further investigation not for designing a dewatering machine.
As described in advance, the physics of ultrasonic mechanisms as atomization, cavitation, and the sponge effect, is relatively unknown. Therefore, in many cases, the only way to have a result for an assumption is a practical experiment.

Some basic laws can be expressed. If the sludge is subjected to high pressure, it may act like a rigid body, and vibrational forces could be reflected back. In contrast, the higher density results in higher sound intensity. So, it may be good to put sludge under pressure. The optimal level of pressure should be determined.

In some musical instruments, it is possible to excite more than one harmonic or mode shapes at the same time. Maybe it could be possible to excite two or more mode shapes simultaneously in sludge.

In some musical instruments when the end of pipes or air columns are open, the energy losses in the form of sound. Maybe the open end of sludge column could help the water extraction associated with the vibrational energy dissipation to the soft boundary or free end.

### 5.3.1 Combining ultrasonic vibration and low frequency oscillation

This idea proposes combining low-frequency high-amplitude vibration and high frequency ultrasound to better distribute the sponge effect, cavitation, and atomization across the sludge material. The idea of low frequency and high amplitude is suggested by the “vibrating screens” used in dewatering.

The function of a low frequency exciter is like vibration screens or resonant acoustic mixers. A resonant acoustic mixer produces micro mixing zones in the material being mixed to promote uniform mixing inside a chamber. Therefore, the low frequency with high amplitude vibration mixes the sludge uniformly, and it could increase the effect of ultrasound more than a single ultrasound transducer. Because of low frequency vibration, sludge particles move about change position uniformly.

Figure 60 depicts a schematic of the proposed system. Here, if the bottom exciter vibrates at 20 Hz, and the upper exciter vibrates ate 20 kHz, during each cycle, a low frequency pressure variation will amplify the pressure a thousand times.

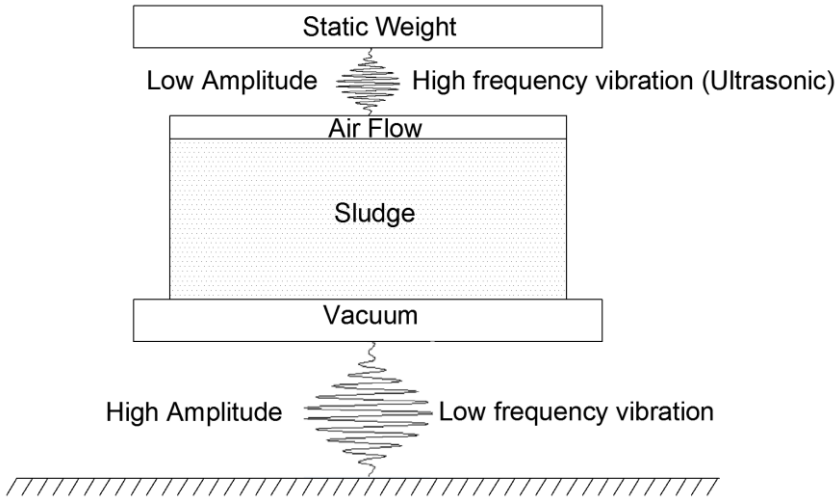


**Figure 60.** Schematic of high frequency ultrasound and low frequency with higher amplitude vibration in addition to pressure deference creator system via air flow and vacuum.

The main idea of using vacuum is to make the pressure difference between two sides of the filter screen. In the sludge side, pressure is about one bar. The other side is subject to vacuum. The pressure difference provides a driving force. Therefore, if in sludge side high pressure is induced and the other side atmospheric pressure with the same ratio of vacuum, the result would be close to each other. Another idea could be making pressure in the sludge side and vacuum in the other side to increase the filtration effect by adding more driving force. The pressure difference idea is coming from the “Drying + ultrasound” practical experiments that use airflow and suction. Pressure difference helps more and faster moisture extraction.

A big improvement in ultrasound assisting dewatering could be activating a mode shape that makes all the particles far from each other in perpendicular direction of the airflow to create a porous material for water migration.

### 5.3.2 Changing the boundary condition

One way to change the mode shape inside a material could be changing the exciter frequency by the factor of two to fill 50% of the pressure and displacement nodes with antinodes, as elaborated in Figure 61. The problem here is that the vibrating plates are tuned in a specific mode of vibration with a certain resonant frequency. Other modes with different resonant frequencies can be excited, but one of the challenges would be to have a driving piezoelectric transducer that also exhibits different excitable modes at the same plate with a specific resonant frequency.

Therefore, a functional solution for the proposed idea could be changing boundary condition based on the laws of standing waves. The similar work in some of the musical instruments is common like Flute.

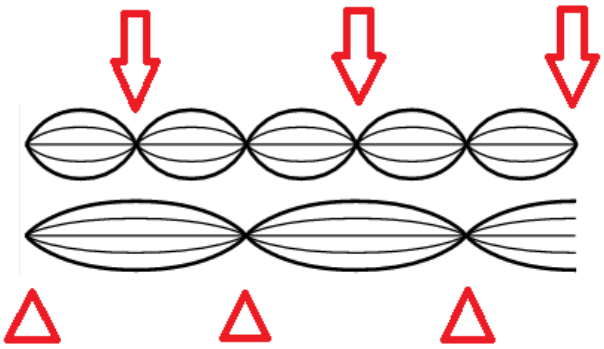

**Figure 61.** Pressure variation graphs in open-open (up) and open-close (down) air columns – The arrows and the triangles show the location of pressure nodes in open-open and open-close columns, respectably [modified, 49].

Based on standing waves principles from “Wave propagation conditions” section, when an open-open column becomes open-close the frequency is divided by two and the wavelength will be doubled, therefore, as illustrated in Figure 61 half of the pressure nodes will become antinodes and the same condition for the displacement nodes. Because of this function the effect of the sponge effect and cavitation at one side and atomization on the other side would be increased.

### 5.3.3 Using two ultrasonic transducer in front of each other

Another solution could be setting up two ultrasonically vibrating plates in front of each other that turn on and off one by one (left plate is on and the right one is off, after for example 1 second, right plate is on and the left one is off). The pressure wave produced would be as shown in Figure 62.

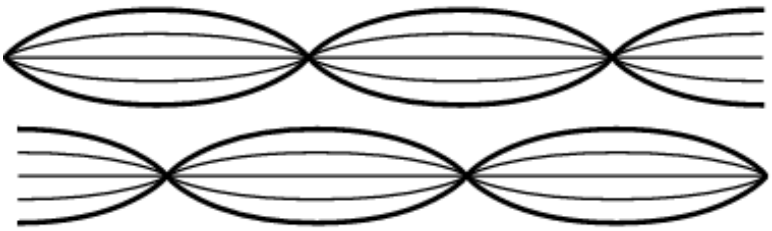

**Figure 62.** (Up) when the left plate is on, (Down) when the right plate is on – In both pressure waves, the other plate that is off acts as a wall that produces the maximum pressure and zero displacement at its border [modified, 49].

The effect of using this method is more than changing boundary condition method as it activates all and not half the nodes. However, about the low frequency and ultrasound vibration combination having an accurate judgment needs practical experiments.

Finally about the frequency level, by taking into account the more effective frequencies for cavitation, sponge effect, and atomization it could be possible that the best frequencies for dewatering process are above or below 20 kHz that means in the audible or ultrasonic range of frequency.

# 6 CONCLUSIONS

This thesis concentrates on physical mechanisms associated with removing capillary and bound water from municipal wastewater sludge. The overriding question is as follows. Using more efficient dewatering and drying methods, can sludge be converted into a useful fuel? In other words, will the energy content of dry sludge be greater than the energy needed to dry it?

Dewatering, which is a purely mechanical process, can remove up to 60% of sludge water content with relatively little energy expenditure, normally thermal drying is hundred times more expensive than mechanical dewatering. The bound water that remains after dewatering, however, is more difficult to remove, and significantly more energy is required to break it loose and remove it. With heat, for example, bound water can be vaporized. In terms of energy consumption, sludge drying is more expensive that pure water.

Therefore, an immediate conclusion is that as much water as possible should be removed via dewatering. The investigation into current dewatering methods revealed that approximately 40% TS content should be achievable using commercially available dewatering equipment. This level of dewatering can possibly be improved upon by enhancing it with high-power ultrasound. Ultrasound has some effective mechanisms that combine to drive water extraction such as atomization, sponge effect, microchannel production, and cavitation. Cavitation helps mechanically and increases initial evaporation rate. It also eradicates harmful bacteria and microorganisms. Theoretically, an ultrasound-enhanced dewatering system could achieve a 60% TS level.

Once all the water has been removed via mechanical processes, an energy efficient means of drying must be used to bring the sludge fuel to its target dryness or TS content. As with dewatering, high-power ultrasound can be used to enhance convective drying, so an ultrasound-enhanced drying process could help to achieve the target TS content. Vacuum may also be helpful. When drying in a vacuum, vaporization of bound water will occur at lower temperatures. An effective and energy efficient drying system could be developed that

uses the waste heat from the sludge-burning furnace boiler to provide the heat of vaporization needed to activate the sludge drying process.

Future research

In the proposed method of combining high and low frequencies, it is beneficial to take advantage of resonance phenomena in oscillating screens and work on vibration patterns that cooperate more with moisture extraction flow. In all the proposed methods, sludge thickness is a key issue for standing wave generation and airflow effectiveness. Another important factor in defining the thickness of sludge under the ultrasound could be the level of damping. The layer cannot so thick that the energy dissipates before fulling penetrating the material. Using a vibration plate on both sides of the material could be an improvement. Additionally, about the sludge layer thickness in relation to the wavelength, it seems necessary to know the wave propagation or the speed of sound and energy damping inside the dewatered sludge to more effectively define the thickness.

A better understanding is needed of the effectiveness of low frequencies and high amplitudes on big particle size and high moisture content and big particle size and high moisture content on frequencies and amplitudes as moisture content drops. Finally, for making pressure difference boundary layer and screening sludge, more research on metallic screen approaches, such as the approach Fournier takes with its rotary press dewatering systems, could be beneficial.

## REFERENCES


1. Reinola, L. Theoretical Basis for Dewatering of Sewage Sludge. In Doctoral school of energy- and geo-technology. Kuressaare, Estonia, 2007. Pp. 157-160.

2. Edwards, A., Arancon Q & Sherman L. Vermiculture Technology: Earthworms, Organic Wastes, and Environmental Management: CRC Press, 2010.

3. Zsirai, I. Sewage Sludge as Renewable Energy. Journal of Residuals Science & Technology, 2011 October. Vol. 8: 4. Pp. 165-179.

4. Zorpas, AA., Vassilis I, Loizidou M & Grigoropoulou H. Particle Size Effects on Uptake of Heavy Metals from Sewage Sludge Compost Using Natural Zeolite Clinoptilolite. Journal of Colloid and Interface Science, 2002 June 1. Vol. 250: 1. Pp. 1-4.

5. EUR-Lex. [web document]. Published 1991, [Referred 2016 March]. Available: http://eur-lex.europa.eu/legal-content/EN/TXT/PDF/?uri=CELEX:31991L0271&from=EN.

6. Smithers. Theguardian. [web document]. Published 2011, [Referred 2016 April]. Available: http://www.theguardian.com/environment/2011/sep/26/thames-water-sewage-flakes-electricity.

7. BioConversion Solutions. [web document]. [Referred 2016 March]. Available in PDF-file: http://www.bioconversionsolutions.com/wp-content/uploads/2013/01/Destroy-Municipal-Sludge.pdf.

8. Final Report of the Commission to Study Methods and Costs of Sewage, Sludge and Septage Disposal, 2007. Report No.: HB 699.

9. Dehydratorjudge, Food Dehydrator Reviews. [web document]. Published 2016, [Referred 2016 March]. Available: http://dehydratorjudge.com/a-brief-history-of-food-drying/.

10. Konnur, Raha S, Tanwar J, Phanikanth S, Pradip & Kapur PC. Data Analysis and Modeling of Constant Pressure Batch Dewatering of Fine Particle Suspensions. Drying Technology, 2008 July 10. Vol. 26: 8. Pp. 1044-1059.

11. Nikku & Ritvanen. Combustion of Dried Sewage Sludge and Municipal Solid Waste. In PAKU plus-Herge, 2015. Lappeenranta.

12. Spellman, FR. Handbook of Water and Wastewater Treatment Plant Operations. 3rd ed.: CRC Press, 2013.

13. Chen, G., Yue PL & Mujumdar AS. Sludge Dewatering and Drying. Drying Technology, 2002. Vol. 20: 4-5.

14. Turovskiy IS & Mathai PK. Wastewater Sludge: Wastewater Bundle, 2006.

15. Scottish Water. [web document]. Published 2008, [Referred 2016 March]. Available: http://www2.scottishwater.co.uk/portal/page/portal/SWE_PGP_INVESTMENT/SWE_PGE_INVESTMENT/WHAT_WWTW_SEA/WHAT_SEA_FACTS/WHAT_SEA_PRI.

16. Mujumdar, S. Handbook of Industrial Drying. Fourth ed.: CRC Press, 2014.

17. Flaga, A. The Aspects of Sludge Thermal Utilization. Kraków, Poland: Cracow University of Technology, Institute of Heat Engineering and Air Protection.

18. Fournier Rotary Press. [web document]. Published 2010, [Referred 2016 April]. Available: http://www.rotary-press.com/.

19. Martínez, Rosas, Morán & Gómez. Effect of Ultrasound Pretreatment on Sludge Digestion and Dewatering Characteristics: Application of Particle Size Analysis Water, 2015 August .

20. Wu, CC., Huang C & Lee. Effects of Polymer Dosage on Alum Sludge Dewatering Characteristics and Physical Properties. Colloids and Surfaces A Physicochemical and Engineering Aspects, 1997 December. Vol. 122: 1.

21. Dombkowski J. Polymer Applications in Biological Treatment Systems. Chemco Products Inc.

22. Asmatulu, R. Air Pressure-Assisted Centrifugal Dewatering of Concentrated Fine Sulfide Particles. International Journal of Rotating Machinery, 2011. 7 p.

23. Glover, P. Fluid Saturation and Capillary Pressure [Fluid Saturation and Capillary Pressure]. [Referred 2016 April]. Available in PDF-file: http://homepages.see.leeds.ac.uk/~earpwjg/PG_EN/CD%20Contents/GGL-66565%20Petrophysics%20English/Chapter%204.PDF.

24. Wills, A & Napier-Munn T. Wills' Mineral Processing Technology: An Introduction to the Practical Aspects of Ore Treatment and Mineral Recovery Seventh , editor.: Butterworth-Heinemann, 2011.

25. liranco. [web document]. [Referred 2016]. Available in PDF-file: http://www.liranco.com/files/ResonanceScreens.29962122.pdf.

26. Richard, WJ. Separation Technologies for Sludge Dewatering. Journal of Hazardous Materials, 2007 July. Vol. 144: 3.

27. DRYCAKE. [web document]. [Referred 2016 May]. Available in PDF-file: http://drycake.com/equipment/dewatering/downloads/centrifuge/DRYCAKE%20CENTRIFUGE%20TECHNOLOGY%20OVERVIEW.pdf.

28. Keller, K & Stahl W. Vibration Screens for Dewatering-Theory and Practice. Minerals and Metallurgical Processing, 1997 February.

29. Elliot, R. Rotary Press Revolutionizes Sludge Compaction [Rotary Press Revolutionizes Sludge Compaction]. [Referred 2016 May]. Available in PDF-file: http://www.tecumseth.com/documents/Rotary%20Press%20Revolutionizes%20Sludge%20Compaction.pdf.

30. Uniwinfilterpress. [web document]. [Referred 2016]. Available: http://www.uniwinfilterpress.com/products/membrane-filter-press/.

31. Filtration + Separation. [web document]. [Referred 2016 April]. Available: http://www.filtsep.com/view/11126/filter-presses-a-review-of-developments-in-automatic-filter-presses/.

32. Mobaraki, M. Municipal Sludge Dewatering and Drying. Lappeenranta: Lappeenranta university of technology, Mechanical Engineering, 2015.

33. Eurostat Statistics Explained. [web document]. Published 2014, [Referred 2015]. Available: http://ec.europa.eu/eurostat/statistics-explained/index.php/Energy_price_statistics#Electricity_prices_for_industrial_consumers.

34. Theweatherprediction. [web document]. [Referred 2016 February]. Available: http://www.theweatherprediction.com/habyhints2/524/.

35. State of Matter. Available: https://docs.google.com/presentation/d/18ArpiuQMU3w1HtMpk7tbgFxSwkzlnTFE4xV99mU_qqw/edit?pref=2&pli=1#slide=id.i19.

36. Hyperphysics. [web document]. [Referred 2016 February]. Available: http://hyperphysics.phy-astr.gsu.edu/hbase/kinetic/vappre.html.

37. Purdue College of Science. [web document]. [Referred 2016 February]. Available: https://www.chem.purdue.edu/gchelp/liquids/vpress.html.

38. ThermExcel. [web document]. [Referred 2016]. Available: http://www.thermexcel.com/english/tables/vap_eau.htm.

39. The Engineering ToolBox. [web document]. [Referred 2016 February]. Available: http://www.engineeringtoolbox.com/water-thermal-properties-d_162.html.

40. Degremont. [web document]. [Referred 2016 March]. Available: http://www.degremont.com/en/know-how/municipal-water-treatment/sludge-treatment/drying/processes/.

41. FY Machinery. [web document]. [Referred 2016 March]. Available: http://rotarydryer.org/products.

42. [Komline-Sanderson Paddle Dryer]. [Referred 2016]. Available in PDF-file: http://www.komline.com/downloads/brochures/KS-SDB_080714.pdf.

43. Wladimir, G. The Delta Dryer, Theoretical and Technological Development of an Energyefficient Dryer for Sludge. Doctoral Dissertation. Delft: Technische Universiteit Delf, 2009.

44. HyperPhysics. [web document]. [Referred 2016 April]. Available: http://hyperphysics.phy-astr.gsu.edu/hbase/sound/earsens.html.

45. Rienstra, SW & Hirschberg A. An Introduction to Acoustics, 2015.

46. Brown, RG. Introductory Physics I: Elementary Mechanics Durham, 2013.

47. HyperPhysics. [web document]. [Referred 2016 April]. Available: http://hyperphysics.phy-astr.gsu.edu/hbase/acoustic/invsqs.html.

48. Crowell, B. Vibrations and Waves: Light and Matter, 2008.

49. The Physics Hypertext Book. [web document]. [Referred 2016 May]. Available: http://physics.info/waves-standing/.

50. Physics 1120: Standing Waves and Sound Level Solutions. [web document]. [Referred 2016]. Available in PDF-file: https://www.kpu.ca/sites/default/files/Faculty%20of%20Science%20%26%20Horticulture/Physics/PHYS%201120%20Standing%20Waves%20and%20Sound%20Level%20Solutions.pdf.

51. Katz, DM. Physics for Scientists and Engineers: Foundations and Connections, Advance Edition: Cengage Learning, 2015.

52. Mulet, A., Ca´rcel JA, Sanjua´n N & Bon J. New Food Drying Technologies – Use of Ultrasound, 2003.

53. Gallego-Juarez, JA., Riera E, de la Fuente Blanco S, Rodrı´guez-Corral G, Acosta-Aparicio VM & Blanco A. Application of High-Power Ultrasound for Dehydration of Vegetables: Processes and Devices. Drying Technology, 2007.

54. De la Fuente-Blanco S, Riera-Franco de Sarabia E, Acosta-Aparicio VM, Blanco-Blanco A & Gallego-Jua´rez J. Food Drying Process by Power Ultrasound. Elsevier, 2006 December. Vol. 122. Pp. 523-527.

55. Gogate, PR. The Use of Ultrasonic Atomization for Encapsulation and Other Processes in Food and Pharmaceutical Manufacturing. In Gallego-Juárez JA, Graff KF. Power Ultrasonics: Applications of High-Intensity Ultrasound. Mumbai, India: Elsevier, 2014. Pp. 911-935.

56. James, A., Vukasinovic B, Smith M & Glezer A. Vibration-induced Drop Atomization and Bursting. Cambridge University Press, 2003. Vol. 476. 28 p.

57. [Dewatering Nonwoven of Cellulose Material with Ultrasonic Technology]. [Referred 2016]. Available: https://www.youtube.com/watch?v=8mOCTruI28Q.

58. Schössler, K. Ultrasound – Fundamentals. In Emerging Technologies, 2011. 85 p.

59. Fernandes FAN & Rodrigues S. Ultrasound Application as Pre-treatment for Drying of Fruits. Fortaleza, Brazil: Universidade Federal do Ceará.

60. Nowacka, M., Tylewicz U, Balestra F, Rosa MD & Witrowa-Rajchert D. Microstructure Changes of Osmodehydrated Kiwifruit Sliced Pretreated with Ultrasound. In InsideFood Symposium. Leuven, Belgium, 2013 April. 5 p.

61. Leong, T., Ashokkumar M & Kentish S. The Fundamentals of Power Ultrasound– A Review. Acoustics Australia, 2011 August. Vol. 39: 2. 10 p.

62. Sorys, P. & Zielewicz-madej E. Ultrasonic Cavitation in Sewage Sludge. Molecular and Quantum Acoustics, 2007: Pp. 247-252.

63. Duan, C., Karnik R, Lu MC & Majumdar A. Evaporation-induced Cavitation in Nanofluidic Channels. PNAS, 2012 March. Vol. 109: 10.

64. The Sonochemistry Centre at Coventry University. [web document]. [Referred 2016 April]. Available: http://www.sonochemistry.info/introdution.htm.

65. Piezoelectric Materials. [web document]. [Referred 2016 April]. Available: http://www.piezomaterials.com/.

66. Gallego-Juárez, JA. & Graff KF. Power Ultrasonics: Applications of High-Intensity Ultrasound: Elsevier, 2014.

67. Gallego-Jua´rez, JA., Rodrı´guez G, Acosta-Aparicio VM, Riera E & Cardoni A. Power Ultrasonic Transducers with Vibrating Plate Radiators. In Gallego-Juárez JA, Graff F. Power Ultrasonics: Applications of High-Intensity Ultrasound. Madrid, Spain: Elsevier, 2014. Pp. 159-193.

68. Gallego-Juárez, JA. Macrosonics: Phenomena, Transducers and Applications. Madrid, Spain: Instituto de Acustica. Report No.: 43.35. 43.25.

69. Riera, E. Solid-liquid Separation Processes Assisted By Power Ultrasound (PU). Madrid, Spain, 2016. 46 p.

70. Gallego-Juarez, JA. High-power Ultrasonic Processing: Recent Developments and Prospective Advances. Elsevier, 2009 January. Vol. 3: 1. Pp. 35-47.

71. Gallego-Juárez, JA., Rodriguez-Corral G, Gálvez Moraleda JC & Yang TS. A New High-Intensity Ultrasonic Technology for Food Dehydration. Madrid: CSIC, Instituto de Acústica.

72. Amazon. [web document]. [Referred 2016]. Available: http://www.amazon.com/Across-International-AT19P7-Stainless-Oil-Filled/dp/B00JXW0YA2/ref=lp_393235011_1_7?s=industrial&ie=UTF8&qid=1463735387&sr=1-7.

73. Shots Health News from NPR. [web document]. [Referred 2015 December]. Available: http://www.npr.org/sections/health-shots/2012/08/08/158447235/why-is-the-worlds-largest-foundation-buying-fake-poop.

74. Rice Knowledge Bank. [web document]. [Referred 2015]. Available: http://www.knowledgebank.irri.org/step-by-step-production/postharvest/drying#guidelines-on-proper-drying.

75. Acoustics and Vibration Animations. [web document]. [Referred 2016]. Available: http://www.acs.psu.edu/drussell/Demos/StandingWaves/StandingWaves.html.

76. Mavko, G. Conceptual Overview of Rock and Fluid Factors that Impact Seismic Velocity and Impedance. Stanford Rock Physics Laboratory.

77. Kotzé, R., Haldenwang R, Fester V & Rössle W. A Feasibility Study of In-line Rheological Characterisation of A Wastewater Sludge Using Ultrasound Technology. Water SA, 2014 October. Vol. 40: 4.

78. Kaleva, E. Optimization of Quantitative High-Frequency Ultrasound Imaging of Articular Cartilage. Doctoral Dissertation. Kuopio: University of Kuopio, Department of Physics, 2009 December.